




Review

Black Phosphorus and its Biomedical Applications

Jane Ru Choi^{1*}, Kar Wey Yong^{2*}, Jean Yu Choi³, Azadeh Nilghaz¹, Yang Lin⁴, Jie Xu⁴, Xiaonan Lu¹

1. Food, Nutrition and Health Programs, Faculty of Land and Food Systems, The University of British Columbia, Vancouver, BC, V6T 1Z4, Canada;
2. Department of Chemical and Petroleum Engineering, Schulich School of Engineering, University of Calgary, Calgary, AB, T2N 1N4, Canada;
3. School of Medicine, Ninewells Hospital and Medical School, University of Dundee, Dundee, DD1 9SY, United Kingdom;
4. Department of Mechanical and Industrial Engineering, University of Illinois at Chicago, Chicago, Illinois 60607, USA.

* Both authors contributed equally to this work.

 Corresponding authors: Xiaonan Lu (xiaonan.lu@ubc.ca), Jane Ru Choi (janeruchoi@gmail.com / janeru.choi@ubc.ca)

© Ivyspring International Publisher. This is an open access article distributed under the terms of the Creative Commons Attribution (CC BY-NC) license (<https://creativecommons.org/licenses/by-nc/4.0/>). See <http://ivyspring.com/terms> for full terms and conditions.

Received: 2017.08.28; Accepted: 2017.10.14; Published: 2018.01.01

Abstract

Black phosphorus (BP), also known as phosphorene, has attracted recent scientific attention since its first successful exfoliation in 2014 owing to its unique structure and properties. In particular, its exceptional attributes, such as the excellent optical and mechanical properties, electrical conductivity and electron-transfer capacity, contribute to its increasing demand as an alternative to graphene-based materials in biomedical applications. Although the outlook of this material seems promising, its practical applications are still highly challenging. In this review article, we discuss the unique properties of BP, which make it a potential platform for biomedical applications compared to other 2D materials, including graphene, molybdenum disulphide (MoS₂), tungsten diselenide (WSe₂) and hexagonal boron nitride (h-BN). We then introduce various synthesis methods of BP and review its latest progress in biomedical applications, such as biosensing, drug delivery, photoacoustic imaging and cancer therapies (i.e., photothermal and photodynamic therapies). Lastly, the existing challenges and future perspective of BP in biomedical applications are briefly discussed.

Key words: black phosphorus, biosensing, drug delivery, photoacoustic imaging, photothermal and photodynamic therapies.

Introduction

Two-dimensional (2D) materials, particularly graphene and its derivative graphene oxide (GO), are increasingly gaining scientific interest due to their excellent mechanical properties and electrical conductivity, large surface area-to-volume ratio and easy functionalization [1, 2]. Similarly, inorganic graphene analogues based upon the transition metal dichalcogenides (TMDs; e.g., molybdenum disulfide (MoS₂)) are of great interest due to their thickness-dependent semiconducting properties [3]. However, the utility of these nanomaterials is limited by a few intrinsic shortcomings, such as a lack of a bandgap in graphene [4] and relatively low carrier mobility in MoS₂ [5]. Taken together, this has motivated the search for alternative 2D materials.

Black phosphorus (BP) has sparked enormous research interest since its discovery in 2014 due to its distinctive structures and useful properties [6]. In the monolayer BP (also known as phosphorene), each

phosphorus atom is covalently bonded with three adjacent phosphorus atoms, thereby forming a bilayer structure along the zigzag direction and puckered structure along the armchair direction [7]. This structural anisotropy contributes to its exceptional properties, including its optical properties [8], mechanical properties [9], electrical conductivity [10], thermoelectric properties [11], and topological features [12], distinguishing it from other 2D materials [e.g., graphene molybdenum disulphide (MoS₂), tungsten diselenide (WSe₂) and hexagonal boron nitride (h-BN)]. Although numerous studies have been conducted to investigate the nano- and opto-electronic applications of BP, including its photonic applications based on its saturable absorption properties [13, 14], little attention has been paid to its potential biomedical applications [15, 16]. This might be mainly due to the lack of stability of black phosphorus when it is exposed to the aqueous

environment or air. Several recent studies have demonstrated the feasibility of synthesizing novel BP nanostructures that are stable in water and air [17-20]. Phosphorus that forms BP is a benign, vital element that acts as a bone constituent, constituting ~1% of the total body weight [21, 22]. As one of the main components of nucleic acids, phosphorus is essential in maintaining human health, leading to a biocompatible material with extensive application potential in the biomedical field [23, 24]. BP has been employed as a biosensing substance for the detection of target analytes (e.g., immunoglobulin G (IgG) [25] and myoglobin (Mb) [26]) due to its inherent electrochemical properties. It has also emerged as a potential agent for drug delivery and anti-tumour therapy owing to its high drug loading efficiency, good biocompatibility, and excellent photothermal and photodynamic properties [27, 28]. Although BP-based biomedical application is still in its infancy with numerous technical challenges remaining to be solved, it may bring novel opportunities for future medical diagnosis and treatment. Therefore, extensive investigation on the potential of BP in biomedical applications, such as biosensing applications and regenerative medicine, would be highly desirable.

The sources of review articles on the fundamental properties of BP and its nano- and opto-electronic applications are extensive and readily available [29-32]. Recently, BP nanomedicine and sensing applications have been reviewed [33, 34]. However, the unique fundamental properties of BP compared to other 2D materials and its advantages for diverse biomedical applications have not yet been clearly discussed. In light of the rising demand for BP as an alternative to graphene-based materials, there is a strong need for a timely and comprehensive review on a wide range of biomedical applications of BP, including colorimetric sensing, fluorescent sensing, electrochemical sensing, field effect transistor sensing, cancer imaging, cancer therapy and drug delivery (Figure 1). In this review article, the unique and fascinating characteristics of BP that contribute to its biomedical applications are first discussed and compared with the properties of other 2D materials (e.g., graphene, MoS₂, WSe₂ and h-BN). The different synthesis methods of BP are then summarized. The advantages of using BP and its biomedical applications in biosensing, bioimaging, drug delivery, and cancer therapy are subsequently reviewed. Finally, the existing challenges and future perspective of BP are briefly discussed.

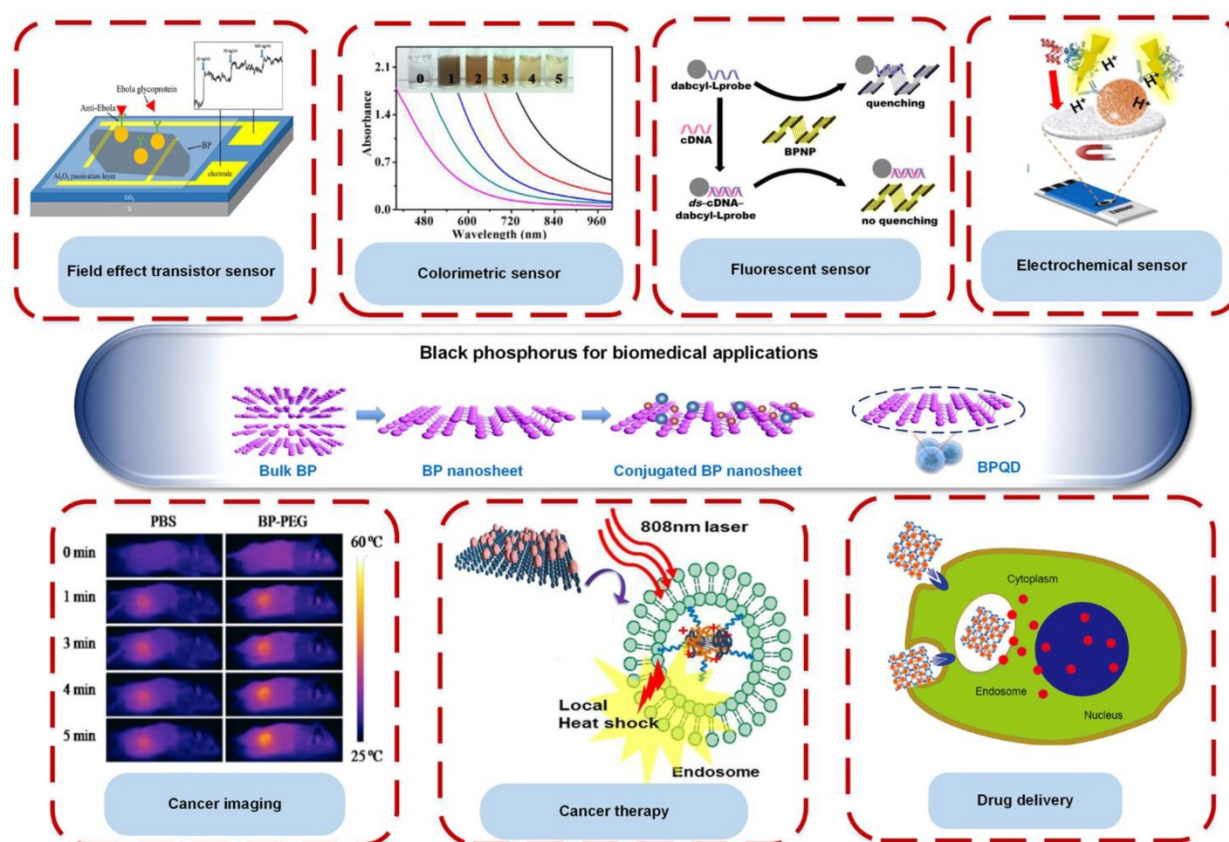


Figure 1. Black phosphorus (BP) as a promising material for biomedical applications. In particular, BP nanosheets and BP quantum dots (BPQD) have been widely used in biosensing, as field effect transistor sensors, colorimetric sensors, fluorescent sensors and electrochemical sensors, cancer imaging, drug delivery and cancer therapy. Reproduced with permission from references: [25], copyright 2017 Elsevier; [16], copyright 2016 ACS publications; [88], copyright 2017 Royal Science Chemistry; [106], copyright 2017 John Wiley & Sons.

Table 1. Summary of the fundamental properties of BP compared to other 2D materials and its advantages for biomedical applications

Type	Black Phosphorus (BP)	Graphene	MoS ₂	WSe ₂	h-BN	Advantages of BP for biomedical applications
Materials / Bandgap (eV)	Semiconductor/ 0.3 - 2.0	Semimetal/ 0	Semiconductor/ 1.2 - 1.8	Semiconductor/ 1.2 - 1.7	Insulator/ 5.9	The wide tuning range of semiconductor BP band gap (by adjusting the layer number) leads to its broad optical absorption across UV, infrared and visible light spectrum, selectively detecting various types of bioanalytes, e.g., DNA, proteins and inorganic ions. This unique optical property allows BP to be used effectively in biosensing, photoacoustic imaging, photodynamic therapy, photothermal therapy, and drug delivery [41].
Carrier mobility (cm ² V ⁻¹ s ⁻¹)	1000	2 × 10 ⁵	10 - 200	140 - 500	-	BP with high carrier mobility is sensitive to electrical perturbation, allowing it to sensitively detect the adsorption and desorption of single gaseous molecules, particularly health hazardous gases, based on the electrical conductivity measurement, making it suitable to be used in gas sensing [43].
ON-OFF current ratio	10 ³ - 10 ⁵	5.5 - 44	10 ⁶ - 10 ⁸	10 ⁴ - 10 ⁶	-	BP with high ON-OFF current ratio can be widely used in field effect transistor-based immunosensors which contributes to its high sensitivity in detecting antigen or antibody based on the electrical resistance measurement [154].
Electrical conduction type	Ambipolar	Ambipolar	n-type	Ambipolar	-	BP exhibits ambipolar characteristic which enable it to detect both the positively and negatively charged biomolecules [154]. This property makes it possible to be applied in biosensing.
Biocompatibility	Yes	Yes	Yes	Yes	Yes	BP exhibits a relatively good biocompatibility and low cytotoxicity; therefore, it is eligible for biomedical applications, especially in photoacoustic imaging, photodynamic and photothermal therapy, and drug delivery
In vivo Biodegradability	Yes	No, requires functionalization	No, requires functionalization	No, requires functionalization	-	BP is readily biodegradable inside human body producing nontoxic intermediates, such as phosphate, phosphite and other P _x O _y upon exposure to water and oxygen, therefore it is safe to be used for <i>in vivo</i> applications, especially for cancer therapy [22].
References	[7, 155]	[36, 156]	[7, 37, 157]	[17, 156]	[38, 158]	

Fundamental properties of black phosphorus for biomedical applications

Compared to other 2D materials, BP has been known as a more favorable material for biomedical applications due to its exceptional properties. A comparison of the unique properties of BP and other 2D materials is summarized in **Table 1**. Generally, graphene shows the highest carrier mobility, but it possesses zero-band gap and low ON-OFF current ratio, which may hinder its application in optical sensing, bio-imaging, and field effect transistor (FET) sensing [35, 36]. MoS₂ and WSe₂ display a high ON-OFF current ratio due to their finite band gap structures, enabling them to be used in FET sensing. However, their narrow range of band gap and low carrier mobility may hinder their applications in many fields (e.g., optical sensor, bio-imaging, and gas sensor) [37]. The 2D hexagonal boron nitride (h-BN) has been known to be a good proton conductor with high electrical resistance, adding its value to water electrolysis and fuel cells. However, its insulating properties limit its other applications (e.g., electrochemical sensing) [38].

BP exhibits a direct and tunable band gap, which is dependent upon the number of layers (i.e., bulk:

~0.3 eV, bilayer: ~1.88 eV, monolayer: ~2.0 eV) [39]. BP can be easily exfoliated into monolayer or few-layer nanosheets due to the weak van der Waals forces among the stacked BP layers [40]. The wide tuning range of the BP band gap allows broad absorption across the visible light, infrared and ultraviolet regions [39], hence contributing to its excellent optical property compared to other 2D materials, which enables fluorescent and colorimetric detection of various types of bioanalytes (e.g., DNA, proteins and inorganic ions). This unique optical property also allows BP to be effectively used in biosensing, photoacoustic imaging, photodynamic therapy, photothermal therapy, and drug delivery [41]. BP also exhibits a high carrier mobility (i.e., 1000 cm²/Vs for a 10 nm thick BP nanoflake) that is superior to TMDs (e.g., MoS₂: 100 cm²/Vs) [39, 42]. This may contribute to its high sensitivity to electrical perturbation, allowing it to detect gases based upon the electrical conductivity measurement [43]. In addition, BP possesses a high ON-OFF current ratio, which supports its application in FET sensing. Its ambipolar characteristic also enables it to detect both positively and negatively charged bioanalytes. The most attractive physical property of BP over other 2D materials is its high in-plane anisotropic properties.

For instance, the physical properties of BP (e.g., structural holes and mass of electrons) have been known to be highly anisotropic because of its band dispersion, a critical factor for anisotropic electrical conductance and electron mobility [44]. These properties enable BP to be used for a variety of biosensing applications [25].

Generally, biocompatibility or toxicity of 2D materials is material-, size- and concentration-dependent [45]. For instance, BP has demonstrated less cytotoxicity than graphene but more cytotoxicity than MoS₂ and WSe₂ [46]. Large BP (~884 nm ± 102.2 nm) was identified to have higher cytotoxicity than small BP (~208.5 nm ± 46.9 nm) [47]. BP was also identified to induce cytotoxicity when applied at a high concentration (>50 µg/mL) [46, 48]. Hence, it is essential to optimize the parameters of BP including, but not limited to, size and concentration before being used for biomedical applications. Overall, BP exhibits relatively low cytotoxicity or good biocompatibility; therefore, it is eligible for biomedical applications. Another distinct property of BP over other 2D materials is its natural *in vivo* biodegradability. BP is readily biodegradable inside the human body, producing nontoxic intermediates, such as phosphate, phosphite and other P_xO_y, upon exposure to water and oxygen; therefore, it is safe to be used for *in vivo* applications [22]. Recent studies have demonstrated that BP nanosheets, particularly those with a small size, have a relatively high reactivity with water and oxygen and are easily degradable in aqueous media [40, 49, 50]. Other 2D materials are not readily degradable and may accumulate inside the human body, which can cause cytotoxicity, and therefore require functionalization with other materials (e.g., polyethylene glycol (PEG), chitosan or glutathione) to enable effective body clearance when they are used for *in vivo* applications [51, 52]. In short, BP exhibits a wide range of tunable bandgap, high carrier mobility, high ON-OFF current ratio, ambipolar characteristic, good biocompatibility, and *in vivo* biodegradability, indicating its greater potential in biomedical applications, including biosensing (optical, FET and gas sensing), photoacoustic imaging, photodynamic and photothermal therapy, and drug delivery over other 2D materials. This will be comprehensively discussed in Section 4.

Synthesis of black phosphorus nanosheets

The fabrication of thin 2D nanostructures can be categorized into “top-down methods” and “bottom-up methods”. In fact, various fabrication methods of BP have been reviewed [53]. Top-down

methods generally involve the exfoliation of bulk material into single or a few layered nanosheets through the application of driving force (e.g., liquid exfoliation and mechanical cleavage). The interlayer distance of two BP layers that are stacked together by weak van der Waals force is ~3.20-3.73 Å. Therefore, compared to other 2D materials, thin layers of BP could be more easily produced by the aforementioned exfoliation methods. On the other hand, bottom-up methods involve the direct fabrication of nanomaterial from a specific precursor through chemical reactions (e.g., wet-chemical methods and chemical vapor deposition (CVD)) [30].

In general, mechanical cleavage and liquid exfoliation represent the most commonly used methods of fabricating BP [30, 54-58]. Mechanical cleavage has been widely used to produce BP nanosheets with high purity (**Figure 2A**). Briefly, the thin flakes are mechanically peeled off from a bulk BP using an adhesive tape [39]. The BP nanosheets are then transferred onto a silicon-based substrate and cleaned with alcohol for removing the residual adhesive tape. The as-prepared BP is then heated up to 180 °C to remove solvent residue [30]. Notably, this method can produce nanosheets with relatively large surface area-to-volume ratio. However, the limitations of this method include the low yield and the limited ability to control size, shape and thickness of BP, which have restricted its practical applications. Another disadvantage of this method is the presence of chemical traces from the adhesive tapes after the process of exfoliation.

To address these challenges, one group has improved the mechanical cleavage method to optimize the deposition of thin BP flakes [40]. The conventional mechanical exfoliation with adhesive tape produces low density BP flakes with trace level of adhesive left on the surface. The authors introduced the cleavage of bulk BP with tape. Then, the thin BP crystallites maintained on the tape was slightly pressed against a polydimethylsiloxane-based substrate. This exfoliation method could substantially increase the yield and reduce the contamination risk of BP flakes. In another study, a combination of mechanical cleavage and plasma-assisted methods were demonstrated to produce a much more stable monolayer BP [59]. To date, the major drawbacks of mechanical exfoliated BP are the difficulty in achieving uniform samples with well-controlled shape, thickness and size and low production yield [53]. Therefore, there is a high demand to develop advanced mass production approaches for practical applications.

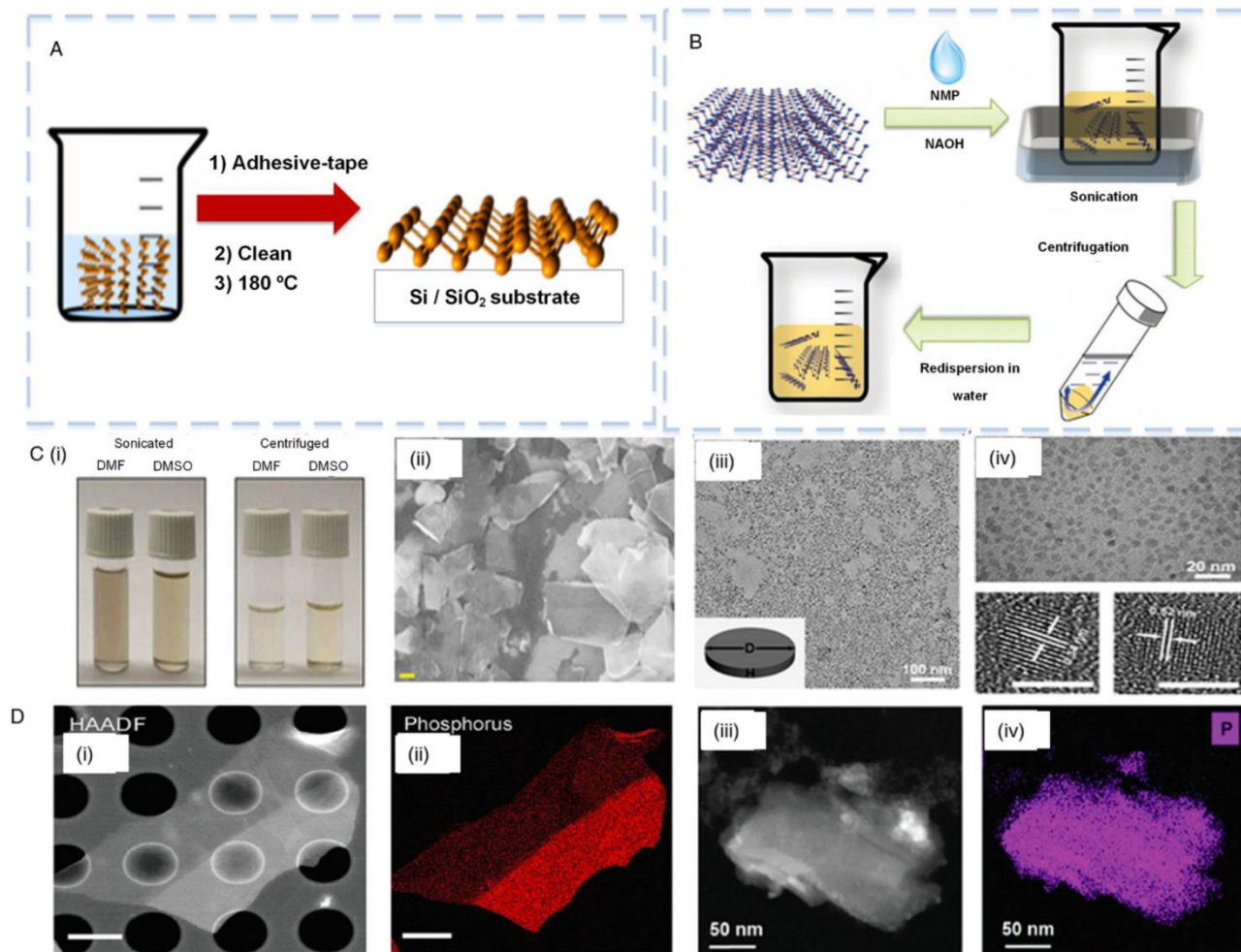


Figure 2. Synthesis of black phosphorus (BP). (A) Mechanical cleavage method and (B) liquid exfoliation method were used to synthesize ultrathin BP nanosheets [58]. (C) (i) Dimethylformamide (DMF) and dimethyl sulfoxide (DMSO) were used as solvents to synthesize BP nanosheets. (ii) Scanning electron microscopy (SEM) image of BP nanosheets [64]. (iii) Transmission electron microscopy (TEM) images of BP quantum dots (BPQDs) synthesized by liquid exfoliation. (iv) Top: enlarged BPQDs image; bottom: high resolution TEM images of BPQDs [65]. (D) (i) Scanning transmission electron microscopy (STEM) image and (ii) energy-dispersive X-ray spectroscopy (EDX) elemental map of BP synthesized by the mechanical cleavage method. (iii) STEM and (iv) EDX elemental map of BP synthesized by the liquid exfoliation method [54]. Reproduced with permission from references: [54], copyright 2014 Royal Science Chemistry; [64], copyright 2015 John Wiley & Sons.

Plasma etching has been introduced, which represents another exfoliation method that can be used to produce monolayer or a few layers of BP through thermal ablation [60]. One group demonstrated the use of an oxygen plasma dry etching method to reduce the thickness of BP flakes layer-by-layer with atomic precision, demonstrating a new method for fabricating high quality, air-stable BP films with a designated number of layers [61]. Combination of the aforementioned method with mechanical cleavage could regulate BP thickness; however, this is not practical in mass production.

Liquid exfoliation has also been extensively used to synthesize ultrathin BP nanosheets [31]. This refers to the exfoliation of mono- to few-layered BP nanosheets and is classified into the following categories: (i) oxidation followed by subsequent dispersion into the solvents, (ii) ion intercalation, (iii)

ion exchange, (iv) shear exfoliation, and (v) ultrasonication-assisted exfoliation, which has been reviewed elsewhere [53]. The most recent approach was ultrasonication-assisted exfoliation that involves ultrasonication of BP in a solvent to cleave the monolayered crystals to few-layered BP nanosheets (**Figure 2B**). This method offers several advantages, including simplicity, low cost, high scalability, and the ability to form thin film and hybrid-composite materials [30, 62]. The first BP liquid exfoliation method was based on surface passivation using N-methyl-2-pyrrolidone (NMP). After that, various types of solvents such as dimethylformamide (DMF), N-cyclohexyl-2-pyrrolidone (CHP), dimethyl sulfoxide (DMSO) and isopropyl alcohol (IPA) were introduced [55, 63]. Particularly, DMF and DMSO have been widely used as solvents for the synthesis of BP nanosheets (**Figure 2C i**) with lateral size of a few

hundred nanometers (**Figure 2C ii**) [64]. In addition to the typical nanosheet structure, quantum dots have also been explored in numerous studies. BP quantum dots (BPQDs) have been known to be a very promising structure due to their size-dependent and tunable electronic and optical properties based upon their crystallographic orientations. BPQDs have also been synthesized using the liquid exfoliation method (**Figure 2C iii, iv**). For example, one study has demonstrated that BPQDs synthesized with this method have a thickness of 1.9 ± 0.9 nm and size of 4.9 ± 1.6 nm [65].

Even though the bulk BP could be effectively exfoliated into BP flakes using those organic solvents, the organic residue could not be removed easily, which might potentially affect the subsequent bio-analysis. More recently, ultrathin BP nanosheets were prepared by exfoliating bulk BP into water instead of solvent [66]. Bulk BP was dispersed in distilled water with argon supply to remove dissolved oxygen molecules, which might cause oxidation, followed by swelling by H₂O and sonication for 8 h. The supernatant was collected after the centrifugation to eliminate the unexfoliated particles. The BP nanosheets could be stable in water without degradation for more than two weeks.

To date, a long duration of sonication process (~10-20 h) is normally required by liquid exfoliation, which could create structural defects and reduce the flake size of BP [54, 67]. For instance, one study has reported that the flake size of BP prepared by NMP was relatively smaller than that of mechanically exfoliated BP (**Figure 2D**). Therefore, it is important to prevent BP from fracturing during the process of sonication in obtaining a large quantity of high quality BP. Ball milling has been introduced to control the particle size of BP [68]. This method could weaken the van der Waals interaction between BP layers with an optimum speed and sonication duration. Additionally, probe-type sonication has also been demonstrated, which requires shorter exfoliation time (~ 5 h) than bath sonication due to its exceptionally high ultrasonic power input, which generates a strong sonication [63, 69]. In short, both mechanical cleavage and liquid exfoliation have showed a lack of ability to produce BP with a precise thickness or size. To address this drawback, it is critical to optimize the centrifugation condition such as centrifugation power [70] and speed [71] to control both size and thickness of BP (e.g., BP nanosheets or BPQDs).

Categorized as one of the liquid exfoliation methods, electrochemical exfoliation has also been introduced to synthesize few-layered BP [60]. The bulk BP crystal was used as a working electrode while a platinum wire was used as a counter electrode. A

voltage was applied between the two electrodes, producing both •OH and •O radicals through the oxidation of water molecules, which accumulate around the BP crystal. The presence of radicals between the consecutive layers of bulk BP weaken the van der Waals interaction between layers, and the production of oxygen gas from the radical oxidation results in the separation of BP layers [72]. Additionally, the electrochemical lithium intercalation method has also been widely used to synthesize 2D materials using layered material as the cathode and lithium foil as the anode [73]. However, this method has not yet been used for BP synthesis due to the fact that upon lithiation process, Li₃P is produced through breakage of the P-P bonds, leading to a phase change and structural instability [74]. Therefore, this challenge has to be addressed prior to its real application. Other liquid exfoliation methods such as microwave-assisted and sheer exfoliation have also been introduced for the synthesis of 2D materials, which offer the potential to produce high-quality and large quantities of BP. The major advantages of electrochemical synthesis methods involve the rapid synthesis process, high crystalline quality of the sample and high production yield [72]. These methods have been reviewed elsewhere [60].

CVD is one of the typical bottom-up methods used to fabricate 2D nanomaterials. This method is performed on a given substrate with precursors at high temperature [30]. As a result, this can produce ultrathin nanomaterials with a large surface area, tunable size and thickness, and excellent crystal quality. Another widely available bottom-up method for preparation of 2D materials is wet-chemical methods [75, 76]. These methods include templated synthesis, solvothermal, hydrothermal and self-assembly of nanocrystals, which offer a low-cost and high-yield production of nanomaterials. Such bottom-up methods have been extensively used in fabricating various nanomaterials, such as graphene and TMDs (e.g., MoS₂, WSe₂) [77-79]. A recent study has demonstrated the synthesis of BP using a wet-chemical method [80]. This approach involves vapor-solid transformation triggered by continuous vaporization condensation, followed by bottom-up assembly growth. In fact, using a bottom-up method is highly challenging, especially to achieve large-scale synthesis of BP accompanied by large-area growth and well-controlled layer thickness. Therefore, in the future, investigating advanced methods for BP synthesis may be promising to explore various biomedical applications.

Surface modification of BP nanomaterials has been demonstrated to provide protection against degradation [32] or for functionality improvement

[81]. For the purpose of improving BP stability upon environmental exposure, BP is usually coated with chemicals (e.g., polylactic-co-glycolic acid, polyethylene glycol, aryl diazonium, titanium sulfonate ligand (TiL_4), TiO_2 and Al_2O_3) or other 2D layered materials, such as graphene and h-BN [20, 32]. For instance, coating of BP nanosheets with Al_2O_3 by atomic layer deposition method mitigated BP degradation, and thus maintained the stability and performance of a BP-based FET sensor [17]. In order to use BP for *in vivo* studies, it can be coordinated with polylactic-co-glycolic acid (by oil-in-water emulsion solvent evaporation method), polyethylene glycol (by high energy mechanical milling method) or TiL_4 to protect BP from degradation *in vivo* by water and oxygen [24, 82, 83]. On the other hand, graphene or h-BN, known to be an excellent gas barrier, can also be used to passivate BP nanosheets to improve its stability [84].

Besides protection, surface modification can also improve the properties of BP and subsequently contribute to its potential use in biomedical applications. For instance, passivation of aryl diazonium on BP nanosheets enhanced the BP ON-OFF current ratio, and thus improved the performance of a BP-based FET sensor [81]. BP nanosheets coated with poly-L-lysine (PLL) facilitated the functionalization of BP with aptamers, which could be used as electrodes to detect biomarkers via electrochemical detection methods [15]. In addition, BP nanosheets functionalized with gold nanoparticles displayed strong catalytic activity in which BP acted as an electron donor for reducing 4-nitrophenol, which is usually used for colorimetric detection of biomarkers [85]. Further, BP nanosheets functionalized with gold and iron oxide nanoparticles showed a higher generation potential of reactive oxygen species (ROS) than that of bare BP upon irradiation with near-infrared (NIR) excitation light source (650 nm), indicating their greater photodynamic capability to promote their application in cancer therapy [86]. To further improve the photodynamic capability of BP, BP nanosheets can be integrated with $\text{NaGdF}_4:\text{Yb,Er@Yb@Nd@Yb}$ upconversion nanoparticles (UCNPs) through electrostatic adsorption. This integration produces a larger amount of ROS upon irradiation with NIR excitation light source at 808 nm than those irradiated at 650 nm and 980 nm, which enhances BP anti-tumour efficiency [87]. The properties of BP and its applications in biomedical fields will be discussed in detail in the next section.

Biomedical applications of black phosphorus

Black phosphorus for sensing

Targeted biomarkers are normally present in an extremely low concentration in clinical blood samples, requiring the development of highly sensitive and specific medical biosensors. BP has been employed as a biosensing platform for sensitive diagnosis of diseases, such as cardiovascular disease and breast cancer. BP nanosheets and BP nanoparticles (BPNPs) have been used for electrical, electrochemical, fluorescent and colorimetric biosensing due to their excellent electrical and electrochemical properties [26], fluorescent nature [88], and electron transfer capability [89, 90].

Field Effect Transistor (FET) biosensors

There have been a number of published research works regarding the FET sensing applications of 2D materials. A recent study demonstrated that a biotin-functionalized few layer MoS_2 FET sensor could be used to detect streptavidin as a model analyte with a detection limit of 1×10^{-4} nM. This sensor had a higher sensitivity than graphene-based sensors (streptavidin with a detection limit of 7×10^{-3} nM) due to its high ON-OFF current ratio [91]. There is no direct comparison between BP and other 2D materials in terms of FET detection of the same target analytes. The special characteristics of BP, such as direct bandgap, high ON-OFF current ratio and high carrier mobility, contributes to its excellent electrical properties, hence making it a good candidate for FET sensing. A recent study demonstrated the utilization of surface-passivated BP as a FET biosensing platform for the detection of IgG [25] (**Figure 3A, B**). The BP-based FET biosensor was developed using BP nanosheets coupled with gold nanoparticle-antibody conjugates through surface functionalization. The mechanically exfoliated BP nanosheets were used as the sensing channel in the FET, with an Al_2O_3 thin film as the dielectric layer for surface passivation. The response of the biosensor was determined by the change in the electrical resistance of BP in the presence of antigen. The antigen-antibody interaction induced a gate potential that changed the drain-source current, showing both high selectivity and sensitivity (with a detection limit of ~ 10 ng/mL) towards human IgG (**Figure 3C, D**). Although this platform showed good stability and high detection sensitivity, its conventional FET setup consists of multiple components (i.e., a semiconductor path as channel, two electrodes as source and drain, and a control electrode as gate) and requires an external electric field, making the fabrication and

operation process complicated [92]. Therefore, an easier design was explored to increase the portability of the sensor for point-of-care use [93].

Compared to other 2D materials, BP may be more suitable for use in FET biosensing due to its highly sensitive electrical properties and functionalizable surface. Importantly, BP shows excellent sensing performance particularly due to its finite band gap and high carrier mobility [93], which allows it to be used for the sensitive detection of other biomolecules. BP-based FET biosensors can potentially be used for rapid and sensitive diagnosis of various diseases, such as cardiovascular diseases and cancer by detecting their specific biomarkers.

Electrochemical biosensor

BP has also been extensively explored in developing electrochemical biosensors [26]. In fact, several 2D materials (e.g., graphene and GO) show great potential in electrochemical sensing due to their good conductivity [94, 95]. For example, GO has been used for sensitive electrochemical detection of leukemia cells at leukemia fraction of $\sim 10^{-11}$ [96] and cervical cancer biomarkers [97] (e.g., carcinoembryonic antigen (CEA) and squamous cell carcinoma antigen (SCCA)) with detection limits of

0.013 ng/mL and 0.010 ng/mL, respectively. Due to its inherent redox properties, BP possesses superior electrochemical properties to further enhance the sensitivity and selectivity of an assay [26]. A recent study reported the label-free electrochemical detection of the cardiac biomarker Mb in serum samples by using a simple aptamer-functionalized BP nanostructured electrode [26] (**Figure 4A i**). The BP nanosheets were modified by cationic polymer PLL that functioned as a linker for further biomolecule interaction with the underlying BP through the nitrogen atoms on PLL. The developed material was subsequently applied for the detection of specific biomarkers. Negatively charged DNA aptamers for Mb were immobilized onto the nanosheets via coulombic interaction between PLL and DNA. Mb can be directly oxidized to iron (III) at the electrode surface by an electron transfer mechanism. This biosensor showed high detection specificity and sensitivity imparted by the synergy of high affinity screened aptamers and enhanced electrochemical properties of the BP (**Figure 4A ii, iii**). It could achieve a lower detection limit (i.e., down to pg level) compared to the reduced GO (rGO)-based biosensor (i.e., ng level).

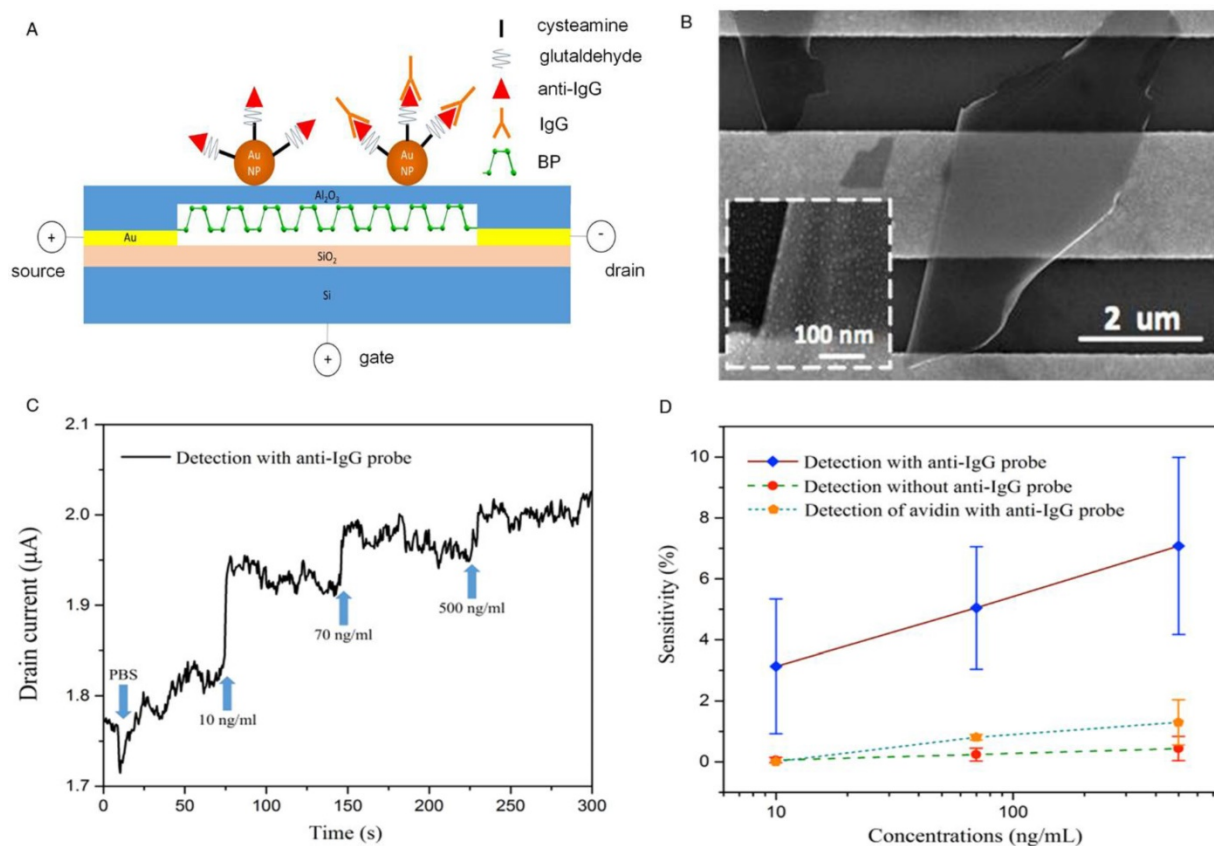


Figure 3. Black phosphorus (BP) as a material of field effect transistors for sensitive detection of target analytes. (A) BP nanosheets were exfoliated and transferred onto the device for the detection of immunoglobulin G (IgG) (B) Scanning electron microscopy image of the mechanically exfoliated BP nanosheets on gold electrodes. (C) Sensor responses to different concentrations of IgG. (D) Specific binding of IgG onto the device shows a higher sensitivity than those without anti-IgG probe and with non-specific protein (i.e., avidin). Reproduced with permission from reference [25], copyright 2017 Elsevier.

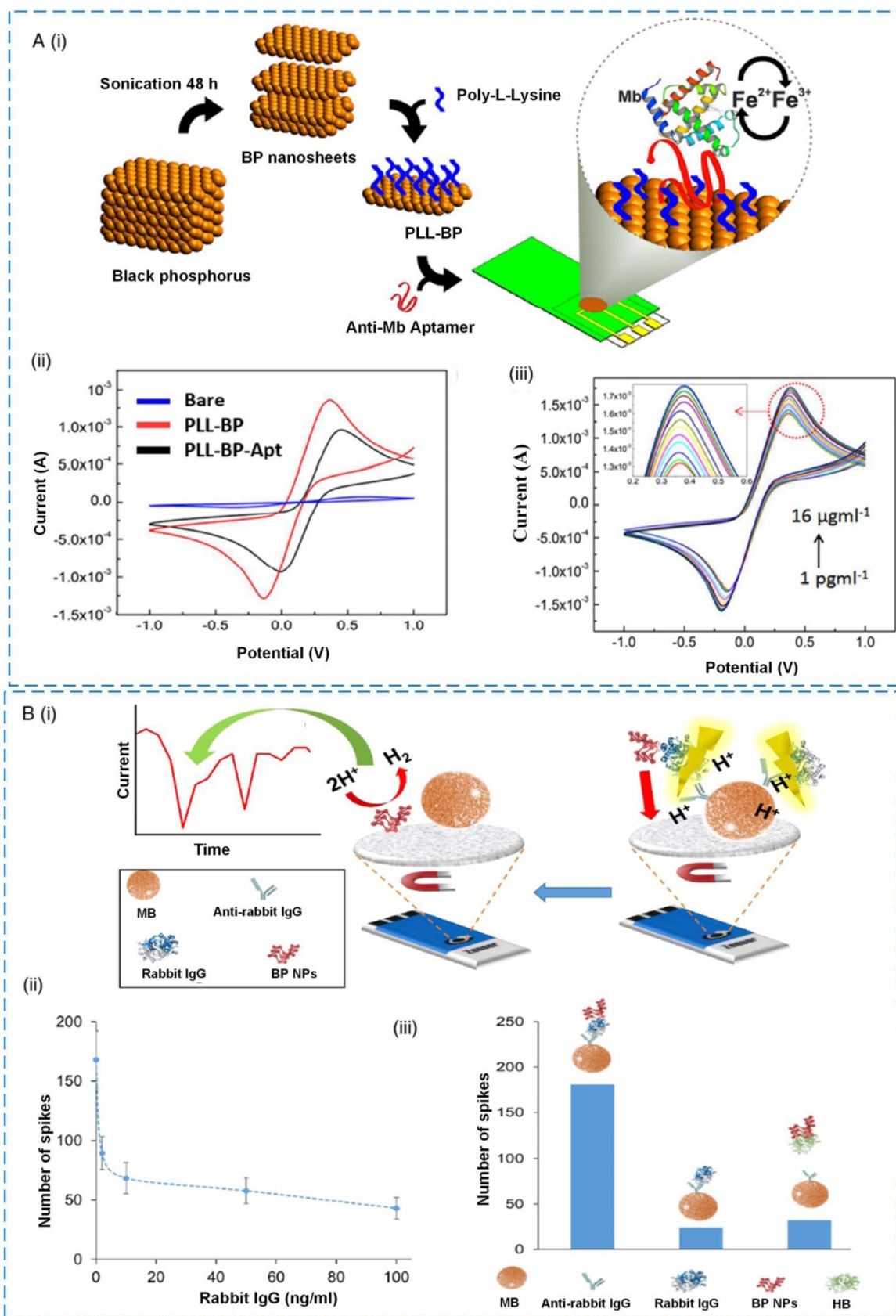


Figure 4. Black phosphorus (BP) as a material for electrochemical detection of target analytes. (A) Aptamer-functionalized BP for electrochemical detection of myoglobin (Mb). (i) Liquid phase exfoliation of BP nanosheets. (ii) Electrochemical response of bare, poly-L-lysine (PLL)-BP and PLL-BP-aptamer modified electrodes with a scan rate of 100 mV/s at potentials ranging from -1 V to +1 V. (iii) Electrochemical response to different concentrations of Mb on PLL-BP aptamer modified sensors [26]. (B) BPNP for electrochemical detection of IgG. (i) BPNP was used as a tag for electrochemical detection based upon nano impact methods. (ii) Chronoamperograms of the competitive immunoassay shows that increasing concentration of IgG reduces the spike count due to competitive binding between IgG-BP and IgG. (iii) The small spike count in the control samples (in the absence of IgG and presence of non-specific protein, hemoglobin (in green)) indicates the good specificity of the assay [16]. Reproduced with permission from references [16, 26], copyright 2016 ACS Publications.

Besides BP nanosheets, developing either BPNPs or BPQDs is of great interest and can lead to versatile applications. For example, BPNPs were used as electrocatalytic tags for the detection of rabbit IgG [16] (**Figure 4B i**). The layered BP microparticles were exfoliated and downsized to nanoparticles with improved electrocatalytic activity for hydrogen evolution reaction. Briefly, the anti-rabbit IgG was conjugated with paramagnetic beads (MB). In the presence of target rabbit IgG, the target was labeled with BPNPs, which was in turn conjugated with MB-anti-rabbit IgG. The addition of acid H_2SO_4 into the complexes resulted in the denaturation of the protein complex and eventually impacted the electrode surface. The concentration of target IgG was determined by electrocatalysis of impacting BPNPs via proton reduction (i.e., hydrogen evolution reaction). This detection strategy was highly sensitive and specific (**Figure 4B ii, iii**), presenting a new concept in biosensing technology.

Another study demonstrated the synthesis of BPQDs with well-crystallized and tunable morphology and size by a high turbulent shear rate produced by a household kitchen blender, which could potentially be used as a humidity sensor for biomedical applications [98]. Upon exposure to water molecules and oxygen, the BP was oxidized to phosphoric acid or phosphorus oxides, which were further ionically dissolved in the moist media to enhance the concentration of H^+ ions [98]. The modulation in ionic conduction of the BPQDs film with the variation in humidity was proposed to contribute to the excellent performance of the BPQDs-based humidity sensor. Due to the water molecule autoionization process (mobile H^+ ion formation), the absorbed moisture layer on the BPQDs surface film can be ionically conductive. Its outstanding humidity sensing performance with high stability and sensitivity suggests its potential use for humidity sensors. In biomedical application, humidity sensors are mandatory to provide an indication of the moisture level for equipment, such as incubators, sterilizers and respiratory equipment for a variety of bioassays.

In short, BP-based biosensors have been reported to achieve more sensitive detection of target analyte(s) compared to other nanomaterial-based biosensors (e.g., graphene-based biosensors) due to their outstanding electrical conductivity, optical response and excellent electrochemical properties [26]. Although other materials (e.g., graphene and rGO) have shown great potential in electrochemical sensing due to their good conductivity, the application of BP could dramatically enhance the detection sensitivity,

and hence are more suitable to be used in electrochemical biosensing.

Fluorescent biosensor

Apart from electrochemical detection, BPNPs have been employed as nanofluorophores in fluorescence-based sensing. Similar to other 2D materials (e.g., GO), BP has excellent optical properties and fluorescent nature, making it a highly efficient fluorescence quencher [88]. In particular, BPQDs offer many advantages, including high quantum yield, good photostability and size-tunable absorption and emission [99]. A variety of parameters including size, shape and composition of BP can be readily manipulated to achieve the desired optoelectrical properties for highly sensitive fluorescence detection [99]. Thus, the quenching efficiency of BP might be superior to the existing organic quenchers.

BPNPs were reported to be used as fluorophores for developing a novel fluorescence-based detection platform for nucleic acids [88] (**Figure 5A**). In the presence of the targeted single-stranded DNA, the DNA would hybridize with a dark quencher label probe, namely dabcyL-L probe, to form a double-stranded DNA complex. This probe is likely to adsorb onto the BPNP fluorophores via hydrophobic interactions and dispersive forces. However, the complex would reduce its affinity to BPNPs and hence would not be adsorbed onto the fluorophore surface. In contrast, the absence of the targeted DNA or double stranded DNA complex would result in photoluminescence quenching of the BPNPs following the adsorption of probe onto the BPNPs, subsequently producing a reduced fluorescence signal. Maximum fluorescence emission was observed at 200 nm, presenting the fluorescent nature of the BPNPs (**Figure 5B**). The proposed detection platform was able to detect DNAs with limits of detection and quantification of 5.9 pM and 19.7 pM, respectively [88] (**Figure 5C**). High specificity was observed with the only positive fluorescence response of BPNPs towards the complementary DNA, whereas negative controls (i.e., mismatched DNA and non-complementary DNA) showed negative results (**Figure 5D**). Although no study has compared the quenching ability of BP with other materials, this finding promotes the investigation of BPNPs as a potential nanomaterial for fluorescent detection of various target analytes, including enzymes, proteins and inorganic ions. For a better understanding of their fluorescent nature, further investigation should involve comparison of the quenching ability of BP with other 2D materials.

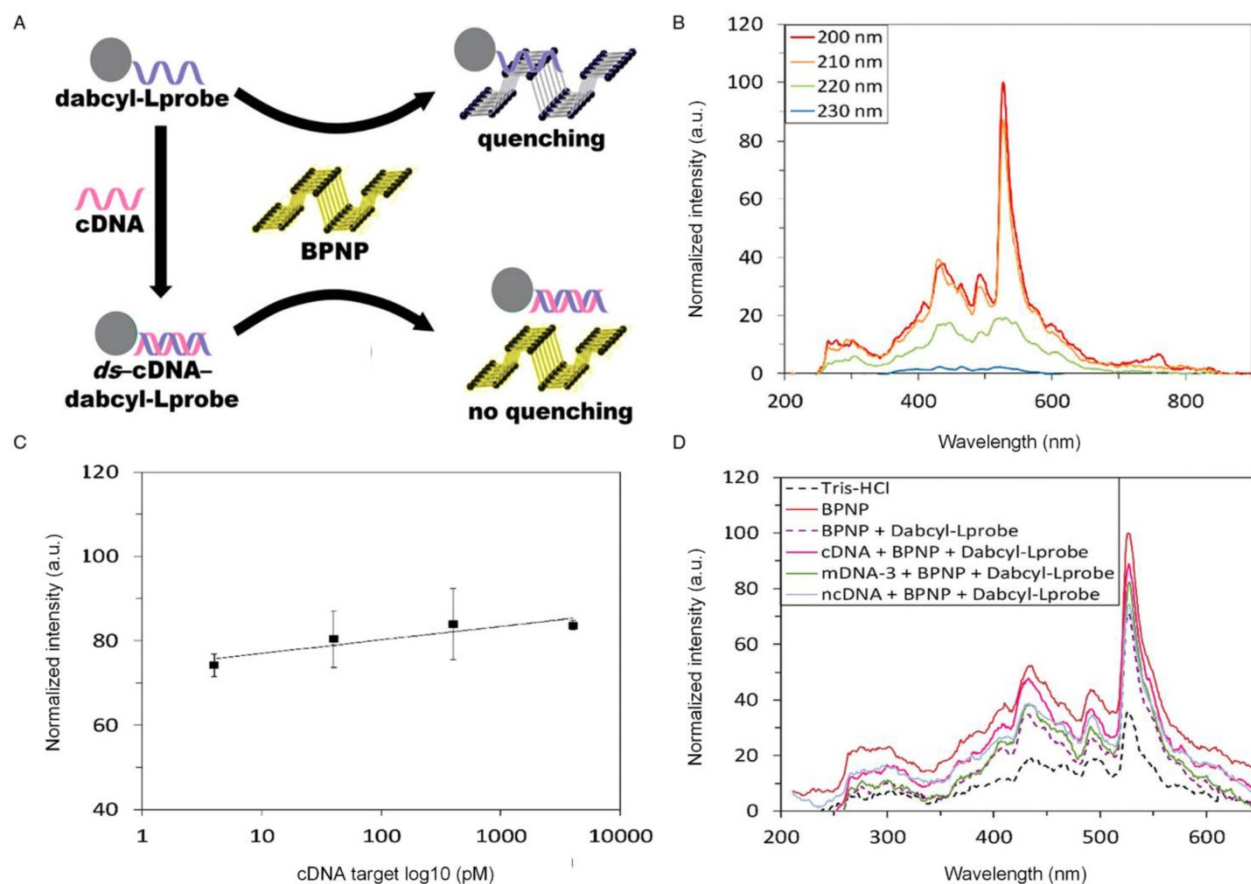


Figure 5. Black phosphorus (BP) as a material for fluorescent detection of target analytes. (A) The fluorescent detection of nucleic acids using BP as fluorophores. (B) The fluorescence emission spectra of BP at 200-230 nm excitation wavelength. The maximum photoluminescence was observed at 200 nm, showing the fluorescent nature of the BP. (C) BP calibration curve at different concentrations of the targeted complementary DNA. (D) The fluorescence response of BP towards the complementary (cDNA), three-base mismatched (mDNA-3) and non-complementary DNA (ncDNA). Reproduced with permission from reference [88], copyright 2017 Royal Science Chemistry.

More recently, a BPNP-based fluorescence detection platform was used for the study of acetylcholinesterase (AChE) activity, which plays a very important role in drug screening, toxin identification and disease diagnosis [100-102]. In general, thiocholine, the product of AChE-catalyzed hydrolysis of acetylthiocholine, can react with 5,5'-dithiobis-(2-nitrobenzoic acid) (DTNB) to produce 2-nitro-5-thiobenzoate anion (TNB) [103]. TNB exhibits considerable spectral overlap with the excitation spectrum of BP and hence it is able to quench the fluorescence of BP [100]. Owing to the unique features of BP such as good photostability, relative high quantum yield and strong green fluorescence, they are highly suitable to be used as a fluorescent biosensing system for the detection of sensitive fluorescent signals. Further experiments using different parameters of BP (e.g., size and shape) as the fluorophores could be beneficial to improving the detection sensitivity and specificity of the targeted component(s) in fluorescent sensing.

Colorimetric biosensor

Besides electrochemical and fluorescent detection, BP has also been demonstrated as a versatile platform for label-free colorimetric detection of targeted biomarkers. Based upon their enhanced AuNP leaching [104] and improved DNA assembly properties [105], some colorimetric detection technologies have been developed using 2D materials (e.g., GO and functionalized graphene). Since different materials may have different outstanding properties, the benefits of BP should be explored for potential improvement in colorimetric sensing.

In fact, BP has demonstrated a lack of stability in water and air, which hinders its optoelectronic applications. The relatively easy degradation of BP could in turn contribute to its strong electron-transfer properties [89, 90], which may potentially improve the detection sensitivity of colorimetric assays. These properties were demonstrated in a recent study using AuNP-decorated few-layered BP (Au-BP) for the detection of cancer biomarkers (i.e., carcinoembryonic antigens (CEA)) in clinical serum samples [106]

(Figure 6A). By mixing hexachloroauric acid and BP, the prepared Au-BP demonstrated a high catalytic activity of reduction of 4-nitrophenol (4-NP). This reaction produced a colorimetric signal from yellow 4-NP to the colorless 4-aminophenol. Upon the addition of anti-CEA antibody, the catalytic activity was switched off due to the adsorption of anti-CEA onto the surface of Au-BP. In the presence of CEA, the formation of antigen-antibody complex switched on the catalytic reaction of Au-BP. This reaction resulted in a good relationship between the intensity of colorimetric signal and the concentration of CEA (Figure 6B, C).

As mentioned previously, BP has a thickness-dependent, direct band gap that is different from graphene [6]. This feature caused the Fermi level of BP to be higher than the reduction potential of AuCl_4^- (i.e., +1.002 V). As a result, a redox reaction was created between BP and AuCl_4^- , allowing spontaneous electron transfer from BP to gold ions that lead to the formation of AuNPs. Therefore, BP presents excellent electron-transfer properties, which could be tuned with different sizes and loading amounts. These properties would enhance the reducibility of catalyst in a redox reaction, and subsequently improve the analytical sensitivity of the developed biosensor. The developed sensor showed a high sensitivity (0.20 pg/mL) and selectivity for the detection of CEA, a biomarker to monitor colon and breast cancer [106]. Therefore, the instability or reducibility of BP could also be used to prepare BP-noble metal hybrids for biosensing applications. Further interesting properties of BP should be explored in future to enhance the performance of colorimetric sensing.

Gas sensor

BP has superior gas sensing performance, which can be applied to detect environmental hazardous gases. In fact, some other 2D materials, such as GO, have been utilized for fabricating gas sensing platforms because their electrical properties are strongly affected by the absorption of gas molecules [107]. The adsorption of gas molecules by BP is stronger than that of other 2D materials, which greatly enhances the electrical properties of BP and subsequently enables the construction of highly sensitive gas sensors [108]. For example, a principle study of the adsorption of NH_3 , CO, CO_2 , NO, and NO_2 onto monolayer BP was conducted. Detection of the gas adsorption by monolayer BP was more sensitive than that of graphene and MoS_2 [109]. The stable conductance and relatively low degradation of BP upon exposure to the gases suggest BP as an excellent gas sensor for biomedical applications.

Another study reported the experimental verification of a BP-based gas sensor and showed increased conduction upon NO_2 exposure (detection sensitivity: 5 ppb) compared to other 2D materials [110]. Due to its reduced charge density, thin BP has a larger surface-to-volume ratio and larger bandgaps than other 2D materials, which is more readily affected by oxidation. Therefore, thicker BP flakes were used to enhance the stability of the device and reduce degradation upon gas exposure [110]. BP was able to maintain its relative stability after sensing, as shown by no significant changes in its Raman spectra before and after exposure to NO_2 . The sensing performance fitted well with the Langmuir Isotherm based upon the adsorption of molecules onto the surface, validating charge transfer as the sensing mechanism. In addition, the conductance increased along with the increase in the concentration of NO_2 . These findings shed light on the importance of the gas sensing characteristics of BP, which can be used in biomedical applications (e.g., breath gas analysis for medical diagnosis).

In short, the sensitivity of BP in detecting the targeted chemical gases was ~20-fold higher than that of graphene and MoS_2 [108]. Compared to other 2D materials, BP shows superior molecular adsorption energy, presenting distinct response to a visible change in the I-V relation either along the zigzag or armchair direction on the basis of the targeted molecules [93, 111]. Moreover, BP has a much higher surface-to-volume ratio due to its puckered structure, maximizing the effect of molecule adsorption [112]. BP also displays less out-of-plane electrical conductance, inducing more sensitive response to the target analytes that are close to the surface of phosphorus [110]. Finally, superior mechanical properties of the P-P bond [9], high operating frequencies [113] and ambipolar behavior of BP [114] are also beneficial to practical applications.

Black phosphorus for cancer imaging

As one of the promising noninvasive cancer imaging technologies, photoacoustic (PA) imaging offers high image contrast and sensitivity, high spatial resolution and depth-resolved 3D imaging. Therefore, it has been shown to be superior to many other traditional optical imaging technologies that facilitate imaging-guided therapy [115]. PA is able to produce high spatial resolution images with optical contrast in the region of 5-6 cm deep in tissues and achieves background-free detection of tumor [116]. Although PA signal originates from the tumor site, the signal intensity is relatively low particularly at the early stage of cancer. Hence, effective exogenous contrast agents, such as NIR absorbing nanomaterials, have

been explored for *in vivo* PA imaging of tumor [117, 118]. For instance, reduced GO was used for *in vivo* PA imaging in theranostic biomedicine due to its intrinsic optical properties [119]. However, the chemical routes for rGO reduction normally require toxic reductants (e.g., hydrazine). Due to P-P stacking interactions, rGO always tends to aggregate, influencing the bioimaging process [120]. To address this issue, functionalized rGO has been introduced to enhance its stability for biomedical imaging [121]. However, alternative materials have been explored to achieve enhanced photodetecting ability while maintaining their stability.

BP has been known as an alternative material for bioimaging due to its unique electronic and optical properties. This material has a tunable band gap ranging from 0.3 eV for bulk to 2.0 eV for a monolayer [7]. Therefore, a multilayer BP could allow photodetection over a broad spectral region [24]. Although BP is very reactive to water and oxygen, surface modification can be performed to enhance its stability. For example, one study demonstrated the surface coordination of a sulfonic ester of titanium ligand (TiL_4) with BPQDs to improve its stability for use as a PA imaging agent for bioimaging of cancer [122] (Figure 7A i, ii). Compared to the bare BPQDs,

TiL_4 -coordinated BPQDs presented higher stability in water dispersion. They also exhibited better PA performance than AuNPs due to their large NIR extinction coefficient. In addition, BPQDs could passively accumulate in tumor at a large concentration via the enhanced permeability and retention effect [122, 123]. Their high spatial resolution in the detection of tumor and excellent sensitivity demonstrate their potential use in clinical applications (Figure 7A iii).

Recently, another study reported the use of polyethylene glycol-(PEG)ylated BPNP for both PA imaging and cancer therapy application [24] (Figure 7B i). The surface polyethylene glycol coating and the partial oxidation of BPNPs allow their excellent stability and solubility in water. *In vivo* studies showed that after 24 h of intravenous injection with PEGylated BPNP, the tumor retained higher intensity of signal compared to kidney and liver (Figure 7B ii). Thus, the nanoparticles have a long retention period in the tumor through the influence of improved permeability and retention, while they can also be readily excreted from the liver and kidney. These properties make them highly suitable for PA imaging of cancer. The role of BP in cancer therapy will be briefly discussed in the next section.

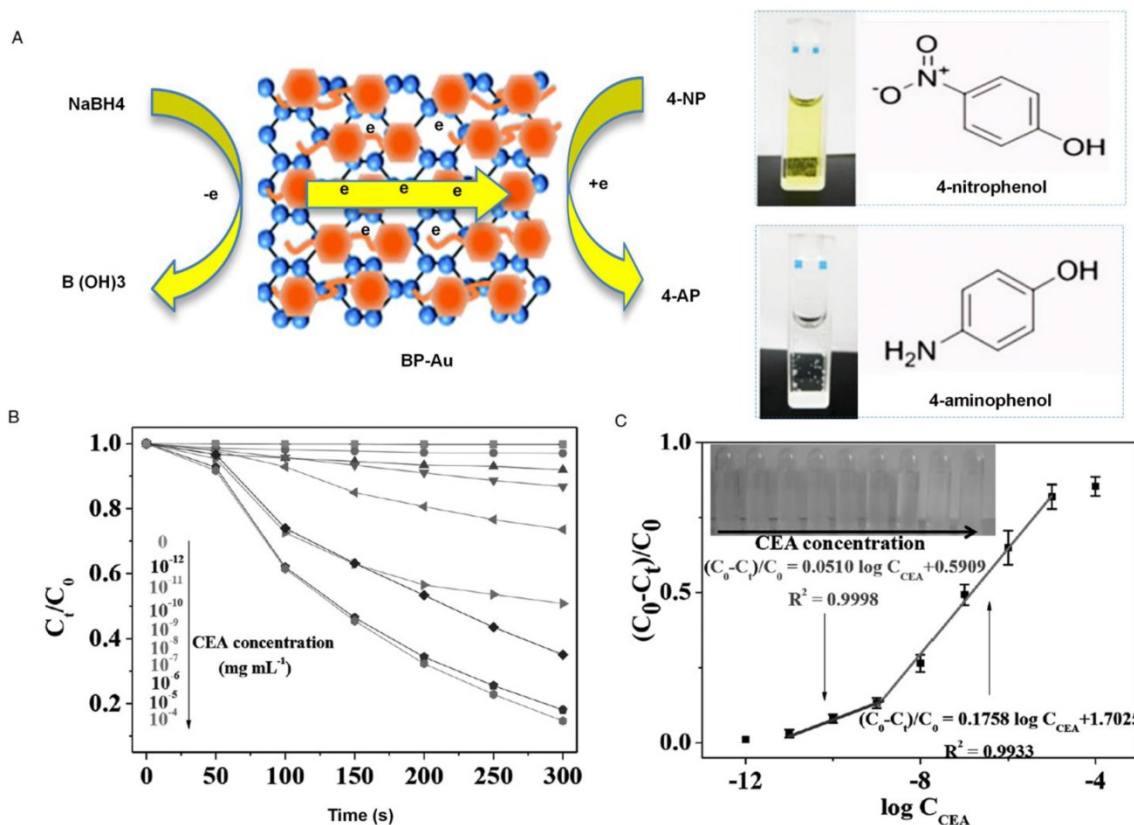


Figure 6. Black phosphorus (BP) as a material for colorimetric detection of target analytes. (A) BP was used as an electron reservoir coupling with gold nanoparticles to enhance catalytic activity towards 4-nitrophenol reduction for the detection of carcinoembryonic antigen (CEA). Mixing of hexachloroauric acid and BP demonstrated a high catalytic activity of 4-nitrophenol (4-NP) reduction, resulting in the color change from yellow 4-NP to the colorless 4-aminophenol. (B) Plot of C_t/C_0 against reaction time in the presence of different concentrations of CEA in human serum. (C) The calibration plot shows a good linear relationship between $(C_0 - C_t)/C_0$ and the logarithm values of the concentration of CEA in serum [106]. Reproduced with permission from reference [106], copyright 2017 John Wiley & Sons.

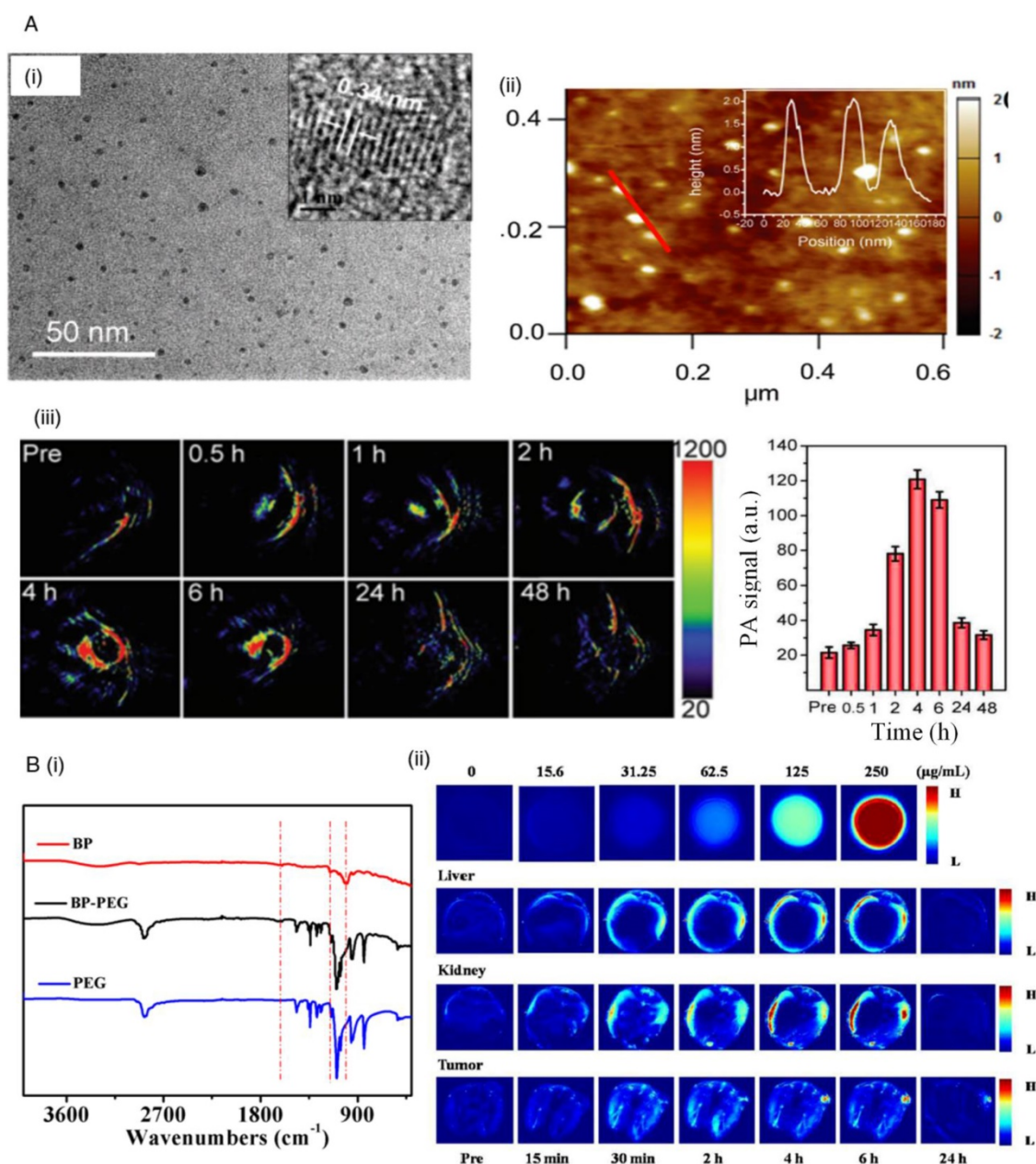


Figure 7. Black phosphorus (BP) as a material for cancer imaging. (A) Titanium ligand (TiL4)-coordinated BPQDs for photoacoustic imaging (PA) of cancer. (i) Transmission electron microscopy and (ii) atomic force microscopy images of TiL4-BPQDs. (iii) Time-dependent PA images and quantitative image analysis of MCF-7 cells in mice after intravenous injection of TiL4-BPQDs. [122] (B) Polyethylene glycol treated (PEGylated) BPNP for PA of cancer. (i) Fourier transform infrared (FT-IR) spectrum of PEGylated BPNP. (ii) *In vivo* PA of PEGylated BPNP solution, liver, kidney and tumour after intravenous injection of PEGylated BPNP at different time points [24]. Reproduced with permission from references: [24], copyright 2016 Elsevier; [122], copyright 2017 John Wiley & Sons.

Black phosphorus for cancer therapy

As an alternative to traditional cancer therapy, BP has been employed in phototherapy, which offers many advantages, such as minimal invasiveness and high therapeutic efficiency [66, 124, 125]. Generally, phototherapy is divided into photothermal therapy (PTT) and photodynamic therapy (PDT) [126]. In PTT, a photothermal agent is used for selective local heating for ablation of cancer cells using NIR light-absorbing agents. In PDT, the treatment is based upon a series of photochemical reactions triggered by

a photosensitizer with specific wavelengths of light. The excitation leads to energy transfer to oxygen molecules in the surrounding areas, which generates cytotoxic ROS that can kill the targeted cancer cells [127]. At present, many nanomaterials (e.g., graphene oxides) have been explored in cancer therapy [128, 129]. BP in particular has scientific interest due to its impressive carrier mobility and tunable band gap that lead to its broad absorption across UV and visible light. Therefore, it could be an excellent photosensitizer to improve PDT and PTT.

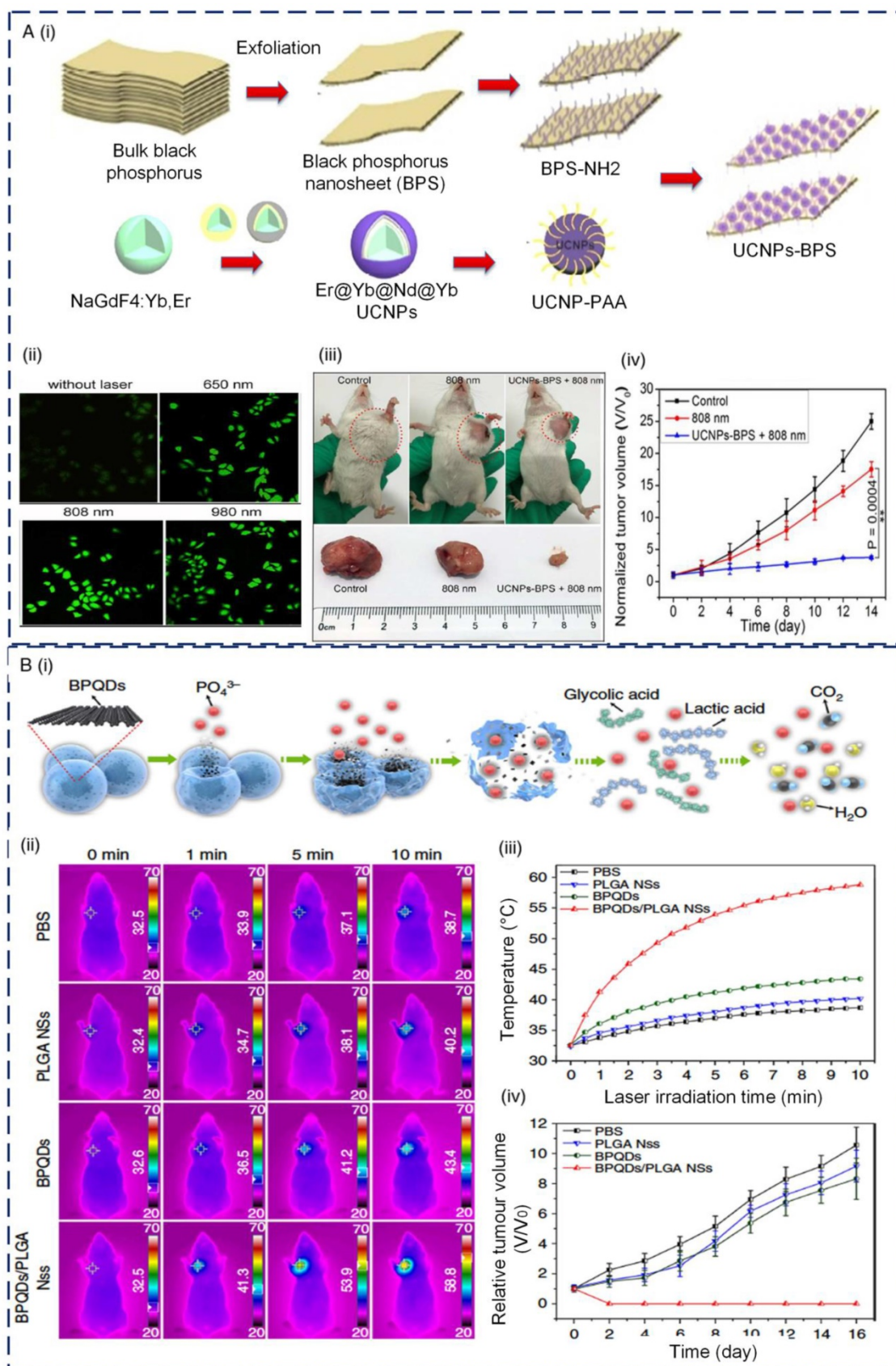


Figure 8. Black phosphorus (BP) as a material for cancer therapy. (A) Upconversion nanoparticle (UCNP)-BP for cancer therapy under 808 nm near infrared (NIR) light irradiation. (i) Synthesis of UCNP-BP. (ii) HeLa cells with UCNP-BP under irradiation at different wavelengths. (iii) Images of tumour in mice on day 14. (iv) The tumor volume of mice over time [87]. (B) Biodegradable BP for photothermal cancer therapy. (i) The process of degradation of the poly (lactic-co-glycolic acid) (PLGA) loaded with BP quantum dots (BPQDs) in the physiological environment. (ii) Infrared thermographic maps. (iii) Upon laser irradiation, the temperature increased in MCF7 breast tumour-bearing mice after injection with PBS, PLGA, BPQDs-PLGA nanospheres (Ns) and BPQDs. (iv) Growth curves of breast tumor (MCF7) in different groups of treated mice under laser irradiation [82]. Reproduced with permission from references: [87], copyright 2016 Royal Science Chemistry; [82], copyright 2016 Nature Publishing Group.

For instance, exfoliated BP nanosheets were reported to be effective photosensitizers for the generation of singlet oxygen that can be applied in PDT of cancer [66]. The photodegradable properties of BP from elemental phosphorus to biocompatible phosphorus oxides under light irradiation illustrate its potential use for cancer therapy. However, the irradiation wavelength within the visible light region possesses strong tissue interference that limits its tissue penetration depth. In addition to therapy, imaging should also be performed to show the theranostic properties of BP. To achieve both functions, a study was conducted to demonstrate a novel multifunctional composite by integrating both NaGdF₄:Yb,Er@Yb@Nd@Yb UCNPs and BP sheets for single 808 nm laser light-mediated photodynamic therapy [87] (Figure 8A i). Combining UCNP and BP allows the activation of BP by a single light source, which produces visible light that could be used as an imaging signal for cell tracking and tumor therapy. Both *in vitro* and *in vivo* studies showed that UCNP-BP with 808-nm light irradiation presented the

highest effect of tumor inhibition. However, the relatively low quantum yield of the up-converted process for the energy donor limits its clinical applications (Figure 8A ii, iii, iv). To this end, a novel nanocomposite that assembles AuNP and iron oxide nanoparticles on BP nanosheets was introduced [130]. By combining both the photothermal effect of AuNP and the tumor targeting and magnetic resonance imaging guiding ability of iron oxide nanoparticles, this platform presents enhanced therapeutic effect. Besides surface modification, it has been demonstrated that the size of BP nanosheets also has an important role in their PTT efficiency [131]. Three different sizes of liquid exfoliated BP nanosheets, namely large BP (~394 nm ± 75 nm), medium BP (~118 nm ± 22 nm) and small BP (~4.5 nm ± 0.6 nm) were used to evaluate their PTT efficiency. Large BP exhibited a significantly higher NIR extinction coefficient, resulting in its greater PTT effect on cancer cells MCF-7 (breast adenocarcinoma) compared to that of medium BP and small BP [131].

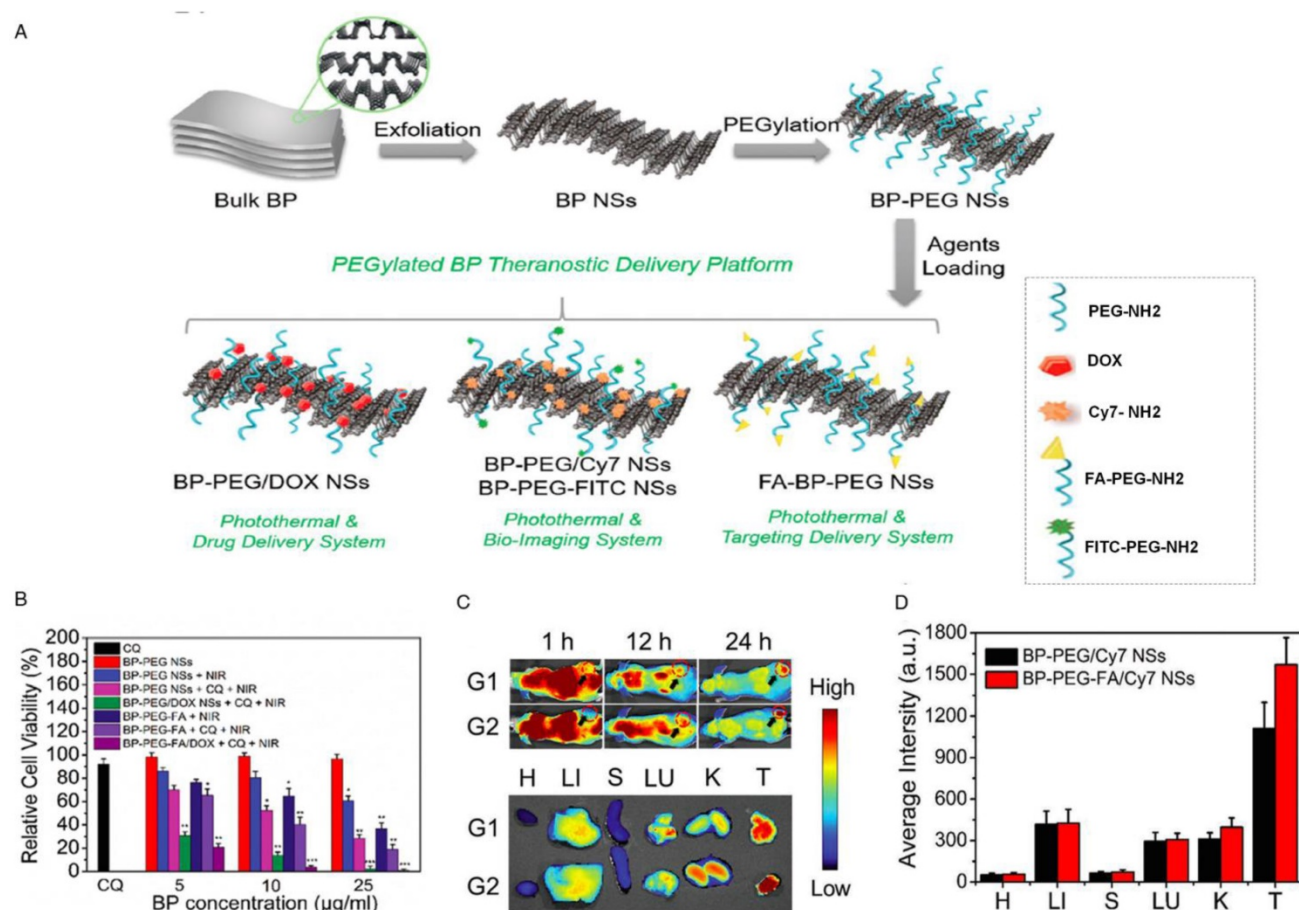


Figure 9. Black phosphorus as a material for drug delivery. (A) BP-based theranostic delivery platform. (B) DOX loaded BP nanosheets enhanced the therapeutic effect by reducing the percentage of viable HeLa cells. (C-D) Strong fluorescence signals were observed in the tumor tissues of both BP-PEG/Cy7 and BP-PEG-FA/Cy7 nanosheets at 24 h post-injection of drugs. (G1: BP-PEG/Cy7 nanosheet group; G2: BP-PEG-FA/Cy7 nanosheet group; H: Heart; LI: Liver; S: Spleen; LU: Lung; K: Kidney; T: Tumor). Reproduced with permission from reference [28], copyright 2017 John Wiley & Sons.

Besides BP nanosheets, BPQDs also offer tremendous potential for cancer therapeutic applications. BPQDs have been known to have a large NIR extinction coefficient, high photothermal conversion efficiency and little cytotoxicity [132, 133]. One recent study demonstrated the potential use of BPQDs for PTT [132]. Due to the broad absorption of BPQDs in the NIR band, remarkable NIR photothermal converting properties were achieved, indicating their potential use for cancer treatment. NIR photoexcitation of BPQDs in the presence of C6 (glioma) and MCF7 cancer cells led to significant cell death, suggesting the potential use of BPQDs as photothermal agents [132]. The enhanced stability of BPQDs after PEG conjugation and the negligible toxicity to different types of cells further suggested their potential use in cancer therapy.

Another recent study reported the synthesis of water-soluble and biocompatible PEGylated BPNPs from stable red phosphorus by the one-pot solvent-less high energy mechanical milling (HEMM) approach [24]. The nanoparticles possessed a uniform size and excellent photostability, biocompatibility and ability to convert NIR light into the heat. The tumor-bearing mice completely recovered after photothermal treatment with PEGylated BPNPs as a heat mediator in comparison to the mice from the control group [24]. The exceptional properties of these nanoparticles suggested their potential use as a theranostic agent for both PA and PTT, offering a perfect solution for accurate diagnosis and treatment of cancer. More recently, a BPQD-based multifunctional nanoplatform was developed for bioimaging and photodynamic/photothermal synergistic cancer therapy [134]. The BPQDs were synthesized through liquid exfoliation and demonstrated high water solubility, excellent biocompatibility and strong NIR absorbance. The effectiveness of PEGylated BPQDs for PTT and PDT was verified with both *in vitro* and *in vivo* studies. Low toxicity of BPQDs was also demonstrated by histological analysis of the main organs of the mice. This study provides tremendous potential for future clinical applications.

Although ultrasmall BPQDs with good biocompatibility and photothermal performance represent potential therapeutic agents, the degradation of their optical properties in the body and rapid renal excretion still restrict their use in clinical applications [82]. To address this challenge, one study demonstrated the use of poly(lactic-co-glycolic acid) (PLGA) loaded with BPQDs to produce BPQDs/PLGA nanospheres for PTT therapy [82] (Figure 8B i). The nanospheres were formed by an oil-in-water emulsion solvent

evaporation method. In fact, PLGA is known as a biocompatible and biodegradable polymer with strong hydrophobicity [135-138]. The degradation rate of nanospheres can be manipulated by adjusting their chemical composition, such as molecular weight and monomer ratio. The integration of PLGA could isolate BPQDs from water and oxygen to improve their photothermal stability and control their degradation rate in the physiological medium. The proposed nanospheres have good biocompatibility and photothermal therapy capability (Figure 8B ii, iii, iv) with negligible toxicity, as shown by highly efficient tumor ablation under NIR laser illumination to achieve a high therapeutic efficiency.

In another study, BP nanosheets functionalized with gold nanoparticles (BP-Au nanosheets) were introduced to enhance NIR for breast cancer PTT [139]. The BP-Au nanosheets exhibit excellent photostability, improved absorption in the NIR region and good photothermal conversion efficiency under irradiation at 808 nm compared to the bare BP nanosheets. Additionally, BP-Au nanosheets also act as effective substrates for surface enhanced Raman scattering (SERS) bioanalysis. Therefore, SERS was performed to monitor the PTT effect and clearly identified molecular fingerprinting features of breast tumors *in vivo*. BP-Au nanosheets with a high SERS activity and excellent PTT effects show promising potential for biomedicine.

Recently, BPQDs were applied as a gene delivery system for cancer therapy. BPQDs were functionalized with polyelectrolyte polymers to deliver lysine-specific demethylase 1 (LSD1) small-interfering RNA (siRNA) into human ovarian teratocarcinoma PA-1 cells [140]. The BPQD-LSD1 siRNA complex exhibited superior transfection efficiency compared to commercial delivery reagents (e.g., Lipofectamine 2000 and Oligofectamine) and was able to inhibit the cell growth rate by >80% in combination with NIR light with negligible cytotoxicity, indicating the potential of applying BPQD for siRNA delivery and cancer therapy.

In fact, the instability of BP has limited its application in cancer therapy. To address this issue, BP nanoflakes were coupled with graphene oxide to create hybrid aerogels that exhibit significantly enhanced photothermal properties and electrical properties [141]. The hybrid gelation of graphene oxide with BP contributes to the stability of BP and protects BP from degradation in ambient conditions, which can eventually aid in biomedical applications (e.g., photothermal therapy for cancer treatment).

Black phosphorus for drug delivery

BP has also been emerging as a suitable

nanomaterial that allows drug delivery and therapeutics. Considering the high surface area of BP, it offers great potential to be used as a superior drug nanocarrier compared to the existing nanomaterials [112]. BP is negatively charged in water with an interlayer distance of $\sim 5.24 \text{ \AA}$ [142]. Therefore, small and positively charged molecular drugs can be encapsulated within the interlayer spaces through electrostatic interactions. One recent study designed a theranostic delivery platform based on BP nanosheets (Figure 9A) [28]. BP nanosheets were functionalized with positively charged PEG-amine to enhance their physiological stability and biocompatibility. The nanoparticles were loaded with the drug doxorubicin (DOX) for chemotherapy and cyanine 7 (Cy7) for *in vivo* NIR imaging. DOX-loaded BP nanosheets enhanced the therapeutic effect by reducing the percentage of viable HeLa cells (Figure 9B). The excellent therapeutic effect of PEGylated BP nanosheets was confirmed, which was attributed to the photothermal effect triggered by the NIR irradiation of BP, DOX-induced chemotherapy and chloroquine (CQ)-mediated inhibition of lysosomes and autophagy. The potential of the PEGylated BP theranostic delivery platform for *in vivo* application was also evaluated via Cy7-loaded BP nanosheets. Strong fluorescence signals were observed in the tumor tissues of both BP-PEG/Cy7 and BP-PEG-FA/Cy7 nanosheets even at 24 h post-injection of drugs, demonstrating good tumor accumulation of the BP delivery platform (Figure 9C, D). Taken together, the BP nanosheets showed promising therapeutic delivery in both *in vitro* and *in vivo* experiments, suggesting their potential use for cancer theranostics.

Similarly, another study also demonstrated BP nanosheet as a drug delivery system with the use of DOX as a model drug [143]. The photothermal effect of BP was validated by the increased temperature under 808 nm laser irradiation, which was stable after six cycles. BP-DOX nanosheets were well dispersed in water without any agglomeration. Fluorescence quenching of DOX was also shown after DOX loading onto BP. BP can carry a high amount of DOX, with a drug loading capacity of 950% in weight, which is higher than other 2D materials (e.g., graphene and MoS_2). This may be due to its higher surface-to-volume ratio and puckered lattice configuration [7].

A BP drug delivery system displayed photo-responsive drug release properties, in which the drug release was accelerated by NIR irradiation at 808 nm [143]. After the intracellular endocytosis of DOX-loaded BP nanosheets under the NIR irradiation, tumour ablation occurred due to the

elevation of the temperature of tumour tissues. At the same time, the loaded drugs could also be triggered to release for enhanced chemotherapy. Since the DOX binding site is in the nucleus and PDT by BP nanosheets normally occurs through the oxidative damage of organelles (e.g., mitochondria) [144, 145], the local hyperthermia increases membrane permeability and promotes drug-organelle interactions. Therefore, the drug release behavior could be enhanced under NIR irradiation at 808 nm [27]. The photodynamic, photothermal and chemotherapy capabilities of BP significantly improve its antitumor efficiency. In short, BP nanosheet is an excellent drug delivery system, as reflected by its improved drug loading efficiency and photo-responsive drug release properties. The drug-loaded BP nanosheet presents significantly enhanced ability to kill cancer cells, demonstrating the efficacy of synergistic chemotherapy, photothermal and photodynamic therapy.

Conclusion and future perspective

In conclusion, this review article presents an overview of the state-of-the-art research in BP for biomedical applications, including biosensing, drug delivery, PA imaging and cancer therapy. The fascinating properties of BP (e.g., direct bandgap, strong structural and functional anisotropy, high conductivity and electron transfer capacity) play a key role in a wide range of biomedical applications. These properties can be further tuned by functionalization and nanostructuring with various substrates. Therefore, BP can be an ideal candidate for practical applications.

Despite the significant advances, research in this area is still in the very early stage compared to other well-explored 2D materials. From a fundamental point of view, producing high-quality and large-scale BP samples remains a challenge. Therefore, a robust and effective method for large-scale production of high-quality BP with precise control over its parameters, including layer number, size, concentration and surface modifications, is essential for potential biomedical applications with negligible toxicity.

Although several studies have demonstrated the use of BP as a highly sensitive gas-sensing platform, its application in medical diagnosis has not been explored yet. Therefore, future studies can also involve breath gas analysis with BP (e.g., measuring the level of breath ammonia and nitric oxide), which enables the detection of various diseases, such as renal disease and asthma [146]. This simple diagnosis approach can potentially substitute conventional methods for the determination of volatile organic

compounds (e.g., spectroscopic methods) [147, 148], which rely on expensive equipment and highly trained personnel. All the phosphorene-based sensing devices have so far only been demonstrated in the laboratory. To make the device commercially available, it is important to deal with the stability of BP during operation to ensure its robustness and reliability for real applications.

Nanomaterials (e.g., graphene) have also been explored in the field of regenerative medicine. To date, the response of cells towards BP substrate in terms of cell functional properties has not been reported yet. Therefore, it would be interesting to study the effect of BP film towards cell functional properties (e.g., viability, proliferation and differentiation) and provide a better understanding of BP-cellular interactions for applications in regenerative medicine. Given that BP possesses greater electrical conductivity than other 2D materials (e.g., graphene) [109], interfacing BP with neurons or cardiomyocytes can potentially explore and stimulate their excellent electrical behavior to facilitate neural or cardiomyocyte regeneration. Synthetic scaffolds such as gelatin methacryloyl (GelMA) hydrogels with tunable stiffness play an important role in extracellular stiffness to convey specific mechanical cues to the adherent cells [149, 150]. Cardiomyocytes seeded on carbon nanomaterials (e.g., carbon nanotube), graphene and GO-polymer hybrid hydrogels have shown improved cardiac tissue morphogenesis, stronger beating behavior and higher spontaneous beating rate compared to those cultured on the pure polymer (e.g., GelMA) [151, 152]. Therefore, it is promising to investigate the potential use of BP-GelMA hybrid hydrogel as a scaffold for neural or cardiac tissue regeneration. As for cancer therapy, alternative 2D materials (i.e., antimonene quantum dots) recently demonstrated superior photothermal conversion efficiency compared to other 2D materials [153]. It would be interesting to study the effect of BP in combination with this 2D material to develop a hybrid therapeutic platform for cancer therapy. With many remaining challenges and opportunities, we envision that there will be more studies focusing on the utilization of BP in biomedical applications in the near future.

Abbreviations

2D: two-dimensional; 4-NP: 4-nitrophenol; AChE: acetylcholinesterase; AuNP: gold nanoparticle; BP: black phosphorus; BPNPs: black phosphorus nanoparticles; BPQDs: black phosphorus quantum dots; CEA: carcinoembryonic antigen; CHP: N-cyclohexyl-2-pyrrolidone; CQ: chloroquine; CVD: chemical vapor deposition; DMF: dimethylfor-

mamide; Cy7: cyanine 7; DMSO: dimethyl sulfoxide; DOX: doxorubicin; FET: field effect transistor; DTNB: 5,5'-dithiobis-(2-nitrobenzoic acid); GelMa: gelatin methacryloyl; GO: graphene oxide; HEMM: high energy mechanical milling; h-BN: hexagonal boron nitride; IgG: immunoglobulin G; IPA: isopropyl alcohol; LSD1: lysine-specific demethylase 1; MB: paramagnetic beads; Mb: myoglobin; MoS₂: molybdenum disulphide; NIR: near infrared; NMP: N-methyl-2-pyrrolidone; PA: photoacoustic; PDT: photodynamic therapy; PEG: polyethylene glycol; PLGA: poly(lactic-co-glycolic acid); PLL: poly-L-lysine; PTT: photothermal therapy; rGO: reduced graphene oxide; ROS: reactive oxygen species; SCCA: squamous cell carcinoma antigen; siRNA: small-interfering RNA; SERS: surface enhanced Raman scattering; TiL₄: titanium sulfonate ligand; TMDs: transition metal dichalogenides; TNB: 2-nitro-5-thiobenzoate anion; UCNPs: upconversion nanoparticles; WSe₂: tungsten selenide.

Acknowledgement

This work was supported by the Natural Sciences and Engineering Research Council of Canada (NSERC RGPIN-2014-05487, CRDPJ 486586-15).

Competing Interests

The authors have declared that no competing interest exists.

References

- Chen Y, Tan C, Zhang H, Wang L. Two-dimensional graphene analogues for biomedical applications. *Chem Soc Rev.* 2015; 44: 2681-701.
- Yan Z, Nika DL, Balandin AA. Thermal properties of graphene and few-layer graphene: applications in electronics. *IET Circuits, Devices & Systems.* 2015; 9: 4-12.
- Rao C, Gopalakrishnan K, Maitra U. Comparative study of potential applications of graphene, MoS₂, and other two-dimensional materials in energy devices, sensors, and related areas. *ACS Appl Mater Interfaces.* 2015; 7: 7809-32.
- Wang X. Graphene nanoribbons: Chemical stitching. *Nat Nanotechnol.* 2014; 9: 875-6.
- Perera MM, Lin M-W, Chuang H-J, Chamlagain BP, Wang C, Tan X, et al. Improved carrier mobility in few-layer MoS₂ field-effect transistors with ionic-liquid gating. *ACS Nano.* 2013; 7: 4449-58.
- Yan Z-Q, Zhang W. The development of graphene-based devices for cell biology research. *Front Mater Sci.* 2014; 8: 107-22.
- Kou L, Chen C, Smith SC. Phosphorene: fabrication, properties, and applications. *J Phys Chem Lett.* 2015; 6: 2794-805.
- Jing Y, Tang Q, He P, Zhou Z, Shen P. Small molecules make big differences: molecular doping effects on electronic and optical properties of phosphorene. *Nanotechnology.* 2015; 26: 095201.
- Wei Q, Peng X. Superior mechanical flexibility of phosphorene and few-layer black phosphorus. *Appl Phys Lett.* 2014; 104: 251915.
- Fei R, Faghaninia A, Soklaski R, Yan J-A, Lo C, Yang L. Enhanced thermoelectric efficiency via orthogonal electrical and thermal conductances in phosphorene. *Nano Lett.* 2014; 14: 6393-9.
- Lv H, Lu W, Shao D, Sun Y. Enhanced thermoelectric performance of phosphorene by strain-induced band convergence. *Phys Rev B.* 2014; 90: 085433.
- Ezawa M. Topological origin of quasi-flat edge band in phosphorene. *New J Phys.* 2014; 16: 115004.
- Luo Z-C, Liu M, Guo Z-N, Jiang X-F, Luo A-P, Zhao C-J, et al. Microfiber-based few-layer black phosphorus saturable absorber for ultra-fast fiber laser. *Opt Express.* 2015; 23: 20030-9.
- Xu Y, Wang Z, Guo Z, Huang H, Xiao Q, Zhang H, et al. Solvothermal synthesis and ultrafast photonics of black phosphorus quantum dots. *Adv Opt Mater.* 2016; 4: 1223-9.

15. Kumar V, Brent JR, Shorie M, Kaur H, Chadha G, Thomas AG, et al. Nanostructured aptamer-functionalized black phosphorus sensing platform for label-free detection of myoglobin, a cardiovascular disease biomarker. *ACS Appl Mater Interfaces*. 2016; 8: 22860-8.
16. Mayorga-Martinez CC, Mohamad Latiff N, Eng AYS, Sofer Zk, Pumera M. Black Phosphorus Nanoparticle Labels for Immunoassays via Hydrogen Evolution Reaction Mediation. *Anal Chem*. 2016; 88: 10074-9.
17. Wood JD, Wells SA, Jariwala D, Chen K-S, Cho E, Sangwan VK, et al. Effective passivation of exfoliated black phosphorus transistors against ambient degradation. *Nano Lett*. 2014; 14: 6964-70.
18. Li P, Zhang D, Liu J, Chang H, Sun Ye, Yin N. Air-stable black phosphorus devices for ion sensing. *ACS Appl Mater Interfaces*. 2015; 7: 24396-402.
19. Zhao Y, Wang H, Huang H, Xiao Q, Xu Y, Guo Z, et al. Surface coordination of black phosphorus for robust air and water stability. *Angew Chem*. 2016; 128: 5087-91.
20. Lee HU, Lee SC, Won J, Son B-C, Choi S, Kim Y, et al. Stable semiconductor black phosphorus (BP)/titanium dioxide (TiO₂) hybrid photocatalysts. *Sci Rep*. 2015; 5.
21. Comber S, Gardner M, Georges K, Blackwood D, Gilmour D. Domestic source of phosphorus to sewage treatment works. *Environ Technol*. 2013; 34: 1349-58.
22. Childers DL, Corman J, Edwards M, Elser JJ. Sustainability challenges of phosphorus and food: solutions from closing the human phosphorus cycle. *Bioscience*. 2011; 61: 117-24.
23. Lee HU, Park SY, Lee SC, Choi S, Seo S, Kim H, et al. Black phosphorus (BP) nanodots for potential biomedical applications. *Small*. 2016; 12: 214-9.
24. Sun C, Wen L, Zeng J, Wang Y, Sun Q, Deng L, et al. One-pot solventless preparation of PEGylated black phosphorus nanoparticles for photoacoustic imaging and photothermal therapy of cancer. *Biomaterials*. 2016; 91: 81-9.
25. Chen Y, Ren R, Pu H, Chang J, Mao S, Chen J. Field-effect transistor biosensors with two-dimensional black phosphorus nanosheets. *Biosens Bioelectron*. 2017; 89: 505-10.
26. Kumar V, Brent JR, Shorie M, Kaur H, Chadha G, Thomas AG, et al. A Nanostructured Aptamer-Functionalised Black Phosphorus Sensing Platform for Label-Free Detection of Myoglobin, a Cardiovascular Disease Biomarker. *ACS ACS Appl Mater Interfaces*. 2016; 8: 22860-8.
27. Chen W, Huang Q, Ou W, Hao Y, Wang L, Zeng K, et al. Self-Reporting Liposomes for Intracellular Drug Release. *Small*. 2014; 10: 1261-5.
28. Tao W, Zhu X, Yu X, Zeng X, Xiao Q, Zhang X, et al. Black Phosphorus Nanosheets as a Robust Delivery Platform for Cancer Theranostics. *Adv Mater*. 2017; 29. doi: 10.1002/adma.201603276.
29. Zhao Y, Chen Y, Zhang Y-H, Liu S-F. Recent advance in black phosphorus: Properties and applications. *Mater Chem Phys*. 2016; 12: 3480-502.
30. Batmunkh M, Bat-Erdene M, Shapter JG. Phosphorene and Phosphorene-Based Materials—Prospects for Future Applications. *Adv Mater*. 2016; 28: 8586-8617.
31. Sorkin V, Cai Y, Ong Z, Zhang G, Zhang Y. Recent Advances in the Study of Phosphorene and its Nanostructures. *Crit Rev Solid State Mater Sci*. 2016: 1-82.
32. Gusmao R, Sofer Z, Pumera M. Black Phosphorus Rediscovered: From Bulk to Monolayer. *Angew Chem*. 2017. 2017; 56: 8052-72.
33. Qian X, Gu Z, Chen Y. Two-dimensional black phosphorus nanosheets for theranostic nanomedicine. *Mater Horiz*. 2017; 4: 800-16.
34. Pumera M. Phosphorene and Black Phosphorus for Sensing and Biosensing. *Trends Anal Chem*. 2017. doi: 10.1016/j.trac.2017.05.002.
35. Geim AK, Novoselov KS. The rise of graphene. *Nat Mater*. 2007; 6: 183-91.
36. Das S, Zhang W, Demarteau M, Hoffmann A, Dubey M, Roelofs A. Tunable transport gap in phosphorene. *Nano Lett*. 2014; 14: 5733-9.
37. Wang QH, Kalantar-Zadeh K, Kis A, Coleman JN, Strano MS. Electronics and optoelectronics of two-dimensional transition metal dichalcogenides. *Nat Nanotechnol*. 2012; 7: 699-712.
38. Song L, Ci L, Lu H, Sorokin PB, Jin C, Ni J, et al. Large scale growth and characterization of atomic hexagonal boron nitride layers. *Nano Lett*. 2010; 10: 3209-15.
39. Liu H, Neal AT, Zhu Z, Luo Z, Xu X, Tománek D, et al. Phosphorene: an unexplored 2D semiconductor with a high hole mobility. *ACS Nano*. 2014; 8: 4033-41.
40. Castellanos-Gomez A, Vicarelli L, Prada E, Island JO, Narasimha-Acharya K, Blanter SI, et al. Isolation and characterization of few-layer black phosphorus. *2D Mater*. 2014; 1: 025001.
41. Ling X, Wang H, Huang S, Xia F, Dresselhaus MS. The renaissance of black phosphorus. *Proc Natl Acad Sci USA*. 2015; 112: 4523-30.
42. Radisavljevic B, Radenovic A, Brivio J, Giacometti iV, Kis A. Single-layer MoS₂ transistors. *Nat Nanotechnol*. 2011; 6: 147-50.
43. Schedin F, Geim A, Morozov S, Hill E, Blake P, Katsnelson M, et al. Detection of individual gas molecules adsorbed on graphene. *Nat Mater*. 2007; 6: 652-5.
44. Fei R, Yang L. Strain-engineering the anisotropic electrical conductance of few-layer black phosphorus. *Nano Lett*. 2014; 14: 2884-9.
45. Lim CT. Biocompatibility and Nanotoxicity of Layered Two-Dimensional Nanomaterials. *ChemNanoMat*. 2017; 3: 5-16.
46. Latiff NM, Teo WZ, Sofer Z, Fisher AC, Pumera M. The cytotoxicity of layered black phosphorus. *Chemistry*. 2015; 21: 13991-5.
47. Zhang X, Zhang Z, Zhang S, Li D, Ma W, Ma C, et al. Size Effect on the Cytotoxicity of Layered Black Phosphorus and Underlying Mechanisms. *Small*. 2017; 13. doi: 10.1002/smll.201701210.
48. Akhavan O, Ghaderi E, Akhavan A. Size-dependent genotoxicity of graphene nanoplatelets in human stem cells. *Biomaterials*. 2012; 33: 8017-25.
49. Island JO, Steele GA, van der Zant HS, Castellanos-Gomez A. Environmental instability of few-layer black phosphorus. *2D Mater*. 2015; 2: 011002.
50. Huang Y, Qiao J, He K, Bliznakov S, Sutter E, Chen X, et al. Degradation of black phosphorus (BP): the role of oxygen and water. *Chem Mater*. 2016; 28: 8330-9.
51. Liu T, Chao Y, Gao M, Liang C, Chen Q, Song G, et al. Ultra-small MoS₂ nanodots with rapid body clearance for photothermal cancer therapy. *Nano Res*. 2016; 9: 3003-17.
52. Wu S-Y, An SSA, Hulme J. Current applications of graphene oxide in nanomedicine. *Int J Nanomedicine*. 2015; 10: 9-24.
53. Dhanabalan SC, Ponraj JS, Guo Z, Li S, Bao Q, Zhang H. Emerging Trends in Phosphorene Fabrication towards Next Generation Devices. *Adv Sci*. 2017; 4(6). doi: 10.1002/adv.201600305.
54. Brent JR, Savjani N, Lewis EA, Haigh SJ, Lewis DJ, O'Brien P. Production of few-layer phosphorene by liquid exfoliation of black phosphorus. *Chem Commun*. 2014; 50: 13338-41.
55. Yasaei P, Kumar B, Foroozan T, Wang C, Asadi M, Tuschel D, et al. High-Quality Black Phosphorus Atomic Layers by Liquid-Phase Exfoliation. *Adv Mater*. 2015; 27: 1887-92.
56. Kang J, Wood JD, Wells SA, Lee J-H, Liu X, Chen K-S, et al. Solvent exfoliation of electronic-grade, two-dimensional black phosphorus. *ACS Nano*. 2015; 9: 3596-604.
57. Woomer AH, Farnsworth TW, Hu J, Wells RA, Donley CL, Warren SC. Phosphorene: synthesis, scale-up, and quantitative optical spectroscopy. *ACS Nano*. 2015; 9: 8869-84.
58. Guo Z, Zhang H, Lu S, Wang Z, Tang S, Shao J, et al. From black phosphorus to phosphorene: basic solvent exfoliation, evolution of Raman scattering, and applications to ultrafast photonics. *Adv Funct Mater*. 2015; 25: 6996-7002.
59. Lu W, Nan H, Hong J, Chen Y, Zhu C, Liang Z, et al. Plasma-assisted fabrication of monolayer phosphorene and its Raman characterization. *Nano Res*. 2014; 7: 853-9.
60. Qiu M, Sun Z, Sang D, Han X, Zhang H, Niu C. Current progress in black phosphorus materials and their applications in electrochemical energy storage. *Nanoscale*. 2017; 9: 13384-403.
61. Pei J, Gai X, Yang J, Wang X, Yu Z, Choi D-Y, et al. Producing air-stable monolayers of phosphorene and their defect engineering. *Nat Commun*. 2016; 7: 10450.
62. Nicolosi V, Chhowalla M, Kanatzidis MG, Strano MS, Coleman JN. Liquid exfoliation of layered materials. *Science*. 2013; 340: 1226419.
63. Hanlon D, Backes C, Doherty E, Cucinotta CS, Berner NC, Boland C, et al. Liquid exfoliation of solvent-stabilised black phosphorus: applications beyond electronics. *Nat Commun*. 2015; 6: 8563.
64. Yasaei P, Kumar B, Foroozan T, Wang C, Asadi M, Tuschel D, et al. High-quality black phosphorus atomic layers by liquid-phase exfoliation. *Adv Mater*. 2015; 27: 1887-92.
65. Zhang X, Xie H, Liu Z, Tan C, Luo Z, Li H, et al. Black phosphorus quantum dots. *Angew Chem Int Ed Engl*. 2015; 54: 3653-7.
66. Wang H, Yang X, Shao W, Chen S, Xie J, Zhang X, et al. Ultrathin black phosphorus nanosheets for efficient singlet oxygen generation. *J Am Chem Soc*. 2015; 137: 11376-82.
67. Batmunkh M, Shearer CJ, Biggs MJ, Shapter JG. Solution processed graphene structures for perovskite solar cells. *J Mater Chem A*. 2016; 4: 2605-16.
68. Sun J, Zheng G, Lee H-W, Liu N, Wang H, Yao H, et al. Formation of stable phosphorus-carbon bond for enhanced performance in black phosphorus nanoparticle-graphite composite battery anodes. *Nano Lett*. 2014; 14: 4573-80.
69. Ryder CR, Wood JD, Wells SA, Hersam MC. Chemically tailoring semiconducting two-dimensional transition metal dichalcogenides and black phosphorus. *ACS Nano*. 2016; 10: 3900-17.
70. Chen Y, Jiang G, Chen S, Guo Z, Yu X, Zhao C, et al. Mechanically exfoliated black phosphorus as a new saturable absorber for both Q-switching and mode-locking laser operation. *Opt Express*. 2015; 23: 12823-33.
71. Woomer AH, Farnsworth TW, Hu J, Wells RA, Donley CL, Warren SC. Phosphorene: synthesis, scale-up, and quantitative optical spectroscopy. *ACS Nano*. 2015; 9: 8869-84.
72. Erande MB, Pawar MS, Late DJ. Humidity sensing and photodetection behavior of electrochemically exfoliated atomically thin-layered black phosphorus nanosheets. *ACS Appl Mater Interfaces*. 2016; 8: 11548-56.
73. Zeng Z, Sun T, Zhu J, Huang X, Yin Z, Lu G, et al. An Effective Method for the Fabrication of Few-Layer-Thick Inorganic Nanosheets. *Angew Chem Int Ed Engl*. 2012; 51: 9052-6.
74. Xia W, Zhang Q, Xu F, Ma H, Chen J, Qasim K, et al. Visualizing the electrochemical lithiation/delithiation behaviors of black phosphorus by in situ transmission electron microscopy. *J Phys Chem C*. 2016; 120: 5861-8.
75. Yoo D, Kim M, Jeong S, Han J, Cheon J. Chemical synthetic strategy for single-layer transition-metal chalcogenides. *J Am Chem Soc*. 2014; 136: 14670-3.
76. Sun Z, Liao T, Dou Y, Hwang SM, Park M-S, Jiang L, et al. Generalized self-assembly of scalable two-dimensional transition metal oxide nanosheets. *Nat Commun*. 2014; 5: 3813.
77. Zhang Y, Zhang L, Zhou C. Review of chemical vapor deposition of graphene and related applications. *Acc Chem Res*. 2013; 46: 2329-39.
78. Ji Q, Zhang Y, Zhang Y, Liu Z. Chemical vapour deposition of group-VIB metal dichalcogenide monolayers: engineered substrates from amorphous to single crystalline. *Chem Soc Rev*. 2015; 44: 2587-602.

79. Lee YH, Zhang XQ, Zhang W, Chang MT, Lin CT, Chang KD, et al. Synthesis of Large-Area MoS₂ Atomic Layers with Chemical Vapor Deposition. *Adv Mater.* 2012; 24: 2320-5.
80. Zhang Y, Rui X, Tang Y, Liu Y, Wei J, Chen S, et al. Wet-Chemical Processing of Phosphorus Composite Nanosheets for High-Rate and High-Capacity Lithium-Ion Batteries. *Adv Energy Mater.* 2016; 6. doi: 10.1002/aenm.201502409.
81. Ryder CR, Wood JD, Wells SA, Yang Y, Jariwala D, Marks TJ, et al. Covalent functionalization and passivation of exfoliated black phosphorus via aryl diazonium chemistry. *Nat Chem.* 2016; 8: 597-602.
82. Shao J, Xie H, Huang H, Li Z, Sun Z, Xu Y, et al. Biodegradable black phosphorus-based nanospheres for in vivo photothermal cancer therapy. *Nat Commun.* 2016; 7: 12967.
83. Sun Z, Zhao Y, Li Z, Cui H, Zhou Y, Li W, et al. TiL4-Coordinated Black Phosphorus Quantum Dots as an Efficient Contrast Agent for In Vivo Photoacoustic Imaging of Cancer. *Small.* 2017; 13. doi: 10.1002/smll.201602896.
84. Doganov RA, O'Farrell EC, Koenig SP, Yeo Y, Ziletti A, Carvalho A, et al. Transport properties of pristine few-layer black phosphorus by van der Waals passivation in an inert atmosphere. *Nat Commun.* 2015; 6: 6647.
85. Peng J, Lai Y, Chen Y, Xu J, Sun L, Weng J. Sensitive Detection of Carcinoembryonic Antigen Using Stability-Limited Few-Layer Black Phosphorus as an Electron Donor and a Reservoir. *Small.* 2017; 13. doi: 10.1002/smll.201603589.
86. Yang D, Yang G, Yang P, Lv R, Gai S, Li C, et al. Assembly of Au Plasmonic Photothermal Agent and Iron Oxide Nanoparticles on Ultrathin Black Phosphorus for Targeted Photothermal and Photodynamic Cancer Therapy. *Adv Funct Mater.* 2017; 27. doi: 10.1002/adfm.201700371.
87. Lv R, Yang D, Yang P, Xu J, He F, Gai S, et al. Integration of Upconversion Nanoparticles and Ultrathin Black Phosphorus for Efficient Photodynamic Theranostics under 808 nm Near-Infrared Light Irradiation. *Chem Mater.* 2016; 28: 4724-34.
88. Yew YT, Sofer Z, Mayorga-Martinez CC, Pumera M. Black phosphorus nanoparticles as a novel fluorescent sensing platform for nucleic acid detection. *Mater Chem Front.* 2017; 1: 1130-6.
89. Sofer Z, Sedmidubský D, Huber Š, Luxa J, Bouša D, Boothroyd C, et al. Layered Black Phosphorus: Strongly Anisotropic Magnetic, Electronic, and Electron-Transfer Properties. *Angew Chem.* 2016; 128: 3443-7.
90. Xu R, Yang J, Zhu Y, Yan H, Pei J, Myint YW, et al. Layer-dependent surface potential of phosphorene and anisotropic/layer-dependent charge transfer in phosphorene-gold hybrid systems. *Nanoscale.* 2016; 8: 129-35.
91. Sarkar D, Liu W, Xie X, Anselmo AC, Mitragotri S, Banerjee K. MoS₂ field-effect transistor for next-generation label-free biosensors. *ACS Nano.* 2014; 8: 3992-4003.
92. Cai B, Huang L, Zhang H, Sun Z, Zhang Z, Zhang G-J. Gold nanoparticles-decorated graphene field-effect transistor biosensor for femtomolar MicroRNA detection. *Biosens Bioelectron.* 2015; 74: 329-34.
93. Cui S, Pu H, Wells SA, Wen Z, Mao S, Chang J, et al. Ultrahigh sensitivity and layer-dependent sensing performance of phosphorene-based gas sensors. *Nat Commun.* 2015; 6: 8632.
94. Zhao H, Peng Z, Wang W, Chen X, Fang J, Xu J. Reduced graphene oxide with ultrahigh conductivity as carbon coating layer for high performance sulfur@reduced graphene oxide cathode. *J Power Sources.* 2014; 245: 529-36.
95. Lei N, Li P, Xue W, Xu J. Simple graphene chemiresistors as pH sensors: fabrication and characterization. *Meas Sci Technol.* 2011; 22: 107002.
96. Akhavan O, Ghaderi E, Hashemi E, Rahighi R. Ultra-sensitive detection of leukemia by graphene. *Nanoscale.* 2014; 6: 14810-9.
97. Wu D, Guo A, Guo Z, Xie L, Wei Q, Du B. Simultaneous electrochemical detection of cervical cancer markers using reduced graphene oxide-tetraethylene pentamine as electrode materials and distinguishable redox probes as labels. *Biosens Bioelectron.* 2014; 54: 634-9.
98. Zhu C, Xu F, Zhang L, Li M, Chen J, Xu S, et al. Ultrafast Preparation of Black Phosphorus Quantum Dots for Efficient Humidity Sensing. *Chemistry.* 2016; 22: 7357-62.
99. Niu X, Li Y, Shu H, Wang J. Anomalous size dependence of optical properties in black phosphorus quantum dots. *J Phys Chem Lett.* 2016; 7: 370-5.
100. Gu W, Yan Y, Pei X, Zhang C, Ding C, Xian Y. Fluorescent black phosphorus quantum dots as label-free sensing probes for evaluation of acetylcholinesterase activity. *Sens Actuators B Chem.* 2017; 250: 601-7.
101. Chang J, Li H, Hou T, Li F. based fluorescent sensor for rapid naked-eye detection of acetylcholinesterase activity and organophosphorus pesticides with high sensitivity and selectivity. *Biosens Bioelectron.* 2016; 86: 971-7.
102. Colovic MB, Krstic DZ, Lazarevic-Pasti TD, Bondzic AM, Vasic VM. Acetylcholinesterase inhibitors: pharmacology and toxicology. *Curr Neuropharmacol.* 2013; 11: 315-35.
103. Moser M, Behnke T, Hamers-Allin C, Klein-Hartwig K, Falkenhagen J, Resch-Genger U. Quantification of PEG-maleimide ligands and coupling efficiencies on nanoparticles with Ellman's reagent. *Anal Chem.* 2015; 87: 9376-83.
104. Shi X, Gu W, Zhang C, Zhao L, Peng W, Xian Y. A label-free colorimetric sensor for Pb²⁺ detection based on the acceleration of gold leaching by graphene oxide. *Dalton Trans.* 2015; 44: 4623-9.
105. Tao Y, Lin Y, Ren J, Qu X. Self-assembled, functionalized graphene and DNA as a universal platform for colorimetric assays. *Biomaterials.* 2013; 34: 4810-7.
106. Peng J, Lai Y, Chen Y, Xu J, Sun L, Weng J. Sensitive Detection of Carcinoembryonic Antigen Using Stability-Limited Few-Layer Black Phosphorus as an Electron Donor and a Reservoir. *Small.* 2017; 13. doi: 10.1002/smll.201603589.
107. Gupta Chatterjee S, Chatterjee S, Ray AK, Chakraborty AK. Graphene-metal oxide nanohybrids for toxic gas sensor: A review. *Sens Actuators B Chem.* 2015; 221: 1170-81.
108. Cho SY, Lee Y, Koh HJ, Jung H, Kim JS, Yoo HW, et al. Superior Chemical Sensing Performance of Black Phosphorus: Comparison with MoS₂ and Graphene. *Adv Mater.* 2016; 28: 7020-8.
109. Kou L, Frauenheim T, Chen C. Phosphorene as a superior gas sensor: Selective adsorption and distinct I-V response. *J Phys Chem Lett.* 2014; 5: 2675-81.
110. Abbas AN, Liu B, Chen L, Ma Y, Cong S, Aroonyadet N, et al. Black phosphorus gas sensors. *ACS Nano.* 2015; 9: 5618-24.
111. Yasaei P, Behranginia A, Foroozan T, Asadi M, Kim K, Khalili-Araghi F, et al. Stable and ultrahigh humidity sensing using stacked black phosphorus flakes. *ACS Nano.* 2015; 9: 9898-905.
112. Ray S. First-principles study of MoS₂, phosphorene and graphene based single electron transistor for gas sensing applications. *Sens Actuators B Chem.* 2016; 222: 492-8.
113. Buscema M, Groenendijk DJ, Blanter SI, Steele GA, van der Zant HS, Castellanos-Gomez A. Fast and broadband photoresponse of few-layer black phosphorus field-effect transistors. *Nano Lett.* 2014; 14: 3347-52.
114. Koenig SP, Doganov RA, Schmidt H, Castro Neto A, Özyilmaz B. Electric field effect in ultrathin black phosphorus. *Appl Phys Lett.* 2014; 104: 103106.
115. Kunjachan S, Ehling J, Storm G, Kiessling F, Lammers T. Noninvasive imaging of nanomedicines and nanotheranostics: principles, progress, and prospects. *Chem Rev.* 2015; 115: 10907-37.
116. Ding K, Zeng J, Jing L, Qiao R, Liu C, Jiao M, et al. Aqueous synthesis of PEGylated copper sulfide nanoparticles for photoacoustic imaging of tumors. *Nanoscale.* 2015; 7: 11075-81.
117. Luke GP, Yeager D, Emelianov SY. Biomedical applications of photoacoustic imaging with exogenous contrast agents. *Ann Biomed Eng.* 2012; 40: 422-37.
118. Kircher MF, De La Zerda A, Jokerst JV, Zavaleta CL, Kempen PJ, Mittra E, et al. A brain tumor molecular imaging strategy using a new triple-modality MRI-photoacoustic-Raman nanoparticle. *Nat Med.* 2012; 18: 829-34.
119. Yang K, Hu L, Ma X, Ye S, Cheng L, Shi X, et al. Multimodal imaging guided photothermal therapy using functionalized graphene nanosheets anchored with magnetic nanoparticles. *Adv Mater.* 2012; 24: 1868-72.
120. Kuila T, Bose S, Mishra AK, Khanra P, Kim NH, Lee JH. Chemical functionalization of graphene and its applications. *Prog Mater Sci.* 2012; 57: 1061-105.
121. Sheng Z, Song L, Zheng J, Hu D, He M, Zheng M, et al. Protein-assisted fabrication of nano-reduced graphene oxide for combined in vivo photoacoustic imaging and photothermal therapy. *Biomaterials.* 2013; 34: 5236-43.
122. Sun Z, Zhao Y, Li Z, Cui H, Zhou Y, Li W, et al. TiL4-Coordinated Black Phosphorus Quantum Dots as an Efficient Contrast Agent for In Vivo Photoacoustic Imaging of Cancer. *Small.* 2017; 13. doi: 10.1002/smll.201602896.
123. Engel M, Steiner M, Avouris P. Black phosphorus photodetector for multispectral, high-resolution imaging. *Nano Lett.* 2014; 14: 6414-7.
124. Sang Y, Zhao Z, Zhao M, Hao P, Leng Y, Liu H. From UV to Near-Infrared, WS₂ Nanosheet: A Novel Photocatalyst for Full Solar Light Spectrum Photodegradation. *Adv Mater.* 2015; 27: 363-9.
125. Zhu C, Yang Y, Luo M, Yang C, Wu J, Chen L, et al. Stabilizing Two Classical Antiaromatic Frameworks: Demonstration of Photoacoustic Imaging and the Photothermal Effect in Metalla-aromatics. *Angew Chem.* 2015; 127: 6279-83.
126. Shibu ES, Hamada M, Murase N, Biju V. Nanomaterials formulations for photothermal and photodynamic therapy of cancer. *J Photochem Photobiol C Photochem Rev.* 2013; 15: 53-72.
127. Li Q, Ruan H, Li H. Nanocarbon materials for photodynamic therapy and photothermal therapy. *Pharm Nanotechnol.* 2014; 2: 58-64.
128. Akhavan O, Ghaderi E, Aghayee S, Fereydooni Y, Talebi A. The use of a glucose-reduced graphene oxide suspension for photothermal cancer therapy. *J Mater Chem.* 2012; 22: 13773-81.
129. Wang Y, Wang H, Liu D, Song S, Wang X, Zhang H. Graphene oxide covalently grafted upconversion nanoparticles for combined NIR mediated imaging and photothermal/photodynamic cancer therapy. *Biomaterials.* 2013; 34: 7715-24.
130. Yang D, Yang G, Yang P, Lv R, Gai S, Li C, et al. Assembly of Au Plasmonic Photothermal Agent and Iron Oxide Nanoparticles on Ultrathin Black Phosphorus for Targeted Photothermal and Photodynamic Cancer Therapy. *Adv Funct Mater.* 2017; 27. doi: 10.1002/adfm.201700371.
131. Fu H, Li Z, Xie H, Sun Z, Wang B, Huang H, et al. Different-sized black phosphorus nanosheets with good cytocompatibility and high photothermal performance. *RSC Adv.* 2017; 7: 14618-24.
132. Sun Z, Xie H, Tang S, Yu XF, Guo Z, Shao J, et al. Ultrasmall black phosphorus quantum dots: synthesis and use as photothermal agents. *Angew Chem.* 2015; 127: 11688-92.
133. Mu X, Wang J, Bai X, Xu F, Liu H, Yang J, et al. Black Phosphorus Quantum Dots Induced Oxidative Stress and Toxicity in Living Cell and Mice. *ACS Appl Mater Interfaces.* 2017; 9: 20399-409.
134. Li Y, Liu Z, Hou Y, Yang G, Fei X, Zhao H, et al. Multifunctional Nanoplatform Based on Black Phosphorus Quantum Dots for Bioimaging and Photodynamic/Photothermal Synergistic Cancer Therapy. *ACS Appl Mater Interfaces.* 2017; 9: 25098-106.

135. Song J, Yang X, Jacobson O, Huang P, Sun X, Lin L, et al. Ultrasmall gold nanorod vesicles with enhanced tumor accumulation and fast excretion from the body for cancer therapy. *Adv Mater.* 2015; 27: 4910-7.
136. Song J, Yang X, Jacobson O, Lin L, Huang P, Niu G, et al. Sequential drug release and enhanced photothermal and photoacoustic effect of hybrid reduced graphene oxide-loaded ultrasmall gold nanorod vesicles for cancer therapy. *ACS Nano.* 2015; 9: 9199-209.
137. Ye F, Barrefelt Å, Asem H, Abedi-Valugerdi M, El-Serafi I, Saghafian M, et al. Biodegradable polymeric vesicles containing magnetic nanoparticles, quantum dots and anticancer drugs for drug delivery and imaging. *Biomaterials.* 2014; 35: 3885-94.
138. Zhang X, Dong Y, Zeng X, Liang X, Li X, Tao W, et al. The effect of autophagy inhibitors on drug delivery using biodegradable polymer nanoparticles in cancer treatment. *Biomaterials.* 2014; 35: 1932-43.
139. Yang G, Liu Z, Li Y, Hou Y, Fei X, Su C, et al. Facile synthesis of black phosphorus-Au nanocomposites for enhanced photothermal cancer therapy and surface-enhanced Raman scattering analysis. *Biomater Sci.* 2017; 5: 2048-55.
140. Yin F, Hu K, Chen S, Wang D, Zhang J, Xie M, et al. Black phosphorus quantum dot based novel siRNA delivery systems in human pluripotent teratoma PA-1 cells. *J Mater Chem B.* 2017; 5: 5433-40.
141. Xing C, Jing G, Liang X, Qiu M, Li Z, Cao R, et al. Graphene oxide/black phosphorus nanoflake aerogels with robust thermo-stability and significantly enhanced photothermal properties in air. *Nanoscale.* 2017; 9: 8096-101.
142. Tayari V, Hemswoth N, Fakhri I, Favron A, Gaurès E, Gervais G, et al. Two-dimensional magnetotransport in a black phosphorus naked quantum well. *Nat Commun.* 2015; 6: 7702.
143. Chen W, Ouyang J, Liu H, Chen M, Zeng K, Sheng J, et al. Black Phosphorus Nanosheet-Based Drug Delivery System for Synergistic Photodynamic/Photothermal/Chemotherapy of Cancer. *Adv Mater.* 2016; 29. doi: 10.1002/adma.201603864.
144. Wang C, Wu C, Zhou X, Han T, Xin X, Wu J, et al. Enhancing cell nucleus accumulation and DNA cleavage activity of anti-cancer drug via graphene quantum dots. *Sci Rep.* 2013; 3: 2852.
145. Zhang C-J, Hu Q, Feng G, Zhang R, Yuan Y, Lu X, et al. Image-guided combination chemotherapy and photodynamic therapy using a mitochondria-targeted molecular probe with aggregation-induced emission characteristics. *Chem Sci.* 2015; 6: 4580-6.
146. Konvalina G, Haick H. Sensors for breath testing: from nanomaterials to comprehensive disease detection. *Acc Chem Res.* 2013; 47: 66-76.
147. Yuan B, Koss A, Warneke C, Gilman JB, Lerner BM, Stark H, et al. A high-resolution time-of-flight chemical ionization mass spectrometer utilizing hydronium ions (H_3O^+ ToF-CIMS) for measurements of volatile organic compounds in the atmosphere. *Atmos Meas Tech.* 2016; 9: 2735-52.
148. Kumar S, Huang J, Abbassi-Ghadi N, Spanel P, Smith D, Hanna GB. Selected ion flow tube mass spectrometry analysis of exhaled breath for volatile organic compound profiling of esophago-gastric cancer. *Anal Chem.* 2013; 85: 6121-8.
149. Tseng Q, Wang I, Duchemin-Pelletier E, Azioune A, Carpi N, Gao J, et al. A new micropatterning method of soft substrates reveals that different tumorigenic signals can promote or reduce cell contraction levels. *Lab chip.* 2011; 11: 2231-40.
150. Gobaa S, Hoehnel S, Lutolf MP. Substrate elasticity modulates the responsiveness of mesenchymal stem cells to commitment cues. *Integr Biol.* 2015; 7: 1135-42.
151. Shin SR, Zihlmann C, Akbari M, Assawes P, Cheung L, Zhang K, et al. Reduced Graphene Oxide-GelMA Hybrid Hydrogels as Scaffolds for Cardiac Tissue Engineering. *Small.* 2016; 12: 3677-89.
152. Shin SR, Jung SM, Zalabany M, Kim K, Zorlutuna P, Kim SB, et al. Carbon-nanotube-embedded hydrogel sheets for engineering cardiac constructs and bioactuators. *ACS Nano.* 2013; 7: 2369-80.
153. Tao W, Ji X, Xu X, Ariful Islam M, Li Z, Chen S, et al. Antimonene Quantum Dots: Synthesis and Application as Near-Infrared Photothermal Agents for Effective Cancer Therapy. *Angew Chem Int Ed Engl.* 2017; 56: 11896-900.
154. de Moraes ACM, Kubota LT. Recent trends in field-effect transistors-based immunosensors. *Chemosensors.* 2016; 4: 20.
155. Li L, Yu Y, Ye GJ, Ge Q, Ou X, Wu H, et al. Black phosphorus field-effect transistors. *Nature Nanotechnol.* 2014; 9: 372-7.
156. Akinwande D, Petrone N, Hone J. Two-dimensional flexible nanoelectronics. *Nat Commun.* 2014; 5.
157. Sahoo S, Gaur AP, Ahmadi M, Guinel MJ-F, Katiyar RS. Temperature-dependent Raman studies and thermal conductivity of few-layer MoS_2 . *J Phys Chem C.* 2013; 117: 9042-7.
158. Jo I, Pettes MT, Kim J, Watanabe K, Taniguchi T, Yao Z, et al. Thermal conductivity and phonon transport in suspended few-layer hexagonal boron nitride. *Nano Lett.* 2013; 13: 550-4.